

## A series of substituted bis-aminotriazines are activators of the natriuretic peptide receptor C.

### Authors and Addresses

Robert J. Smith,<sup>1‡</sup> Cristina Perez-Tenero,<sup>2‡</sup> Dan Conole,<sup>1</sup> Capucine Martin,<sup>2</sup> Sam Myers,<sup>1</sup> Adrian Hobbs,<sup>2\*</sup> David Selwood.<sup>1\*</sup>

<sup>1</sup> Wolfson Institute for Biomedical Research,  
University College London,  
London, UK

<sup>2</sup> William Harvey Research Institute, Barts & The London School of  
Medicine, Queen Mary University of London, Charterhouse Square, London EC1M 6BQ, UK

‡indicates equal contribution

\*corresponding author

### Abstract

C-type natriuretic peptide (CNP) is involved in the regulation of vascular homeostasis, which is at least partly mediated through agonism of natriuretic peptide receptor C (NPRC), loss of this signalling has been associated with vascular dysfunction, as such NPRC is a novel therapeutic target to treat cardiovascular diseases. A series of novel small molecules has been designed and synthesised, structure activity relationships were evaluated by a surface plasmon resonance binding assay. Biological activity of hit compounds was confirmed through organ bath assays measuring vascular relaxation, which was shown to be NPR-C dependant. Lead compound **1** was identified as a potent agonist ( $EC_{50} \sim 1 \mu\text{M}$ ) with promising *in vivo* pharmacokinetic properties.

### Introduction

The natriuretic peptide receptors (NPR) are a class of transmembrane receptors found in several tissues including the brain, bone, vascular and cardiac tissue, and are divided into three known isoforms, NPR-A, NPR-B and NPR-C.<sup>1-2</sup> NPR-A and NPR-B are coupled to a guanylyl cyclase domain, and upon ligand binding levels of cyclic GMP are increased.<sup>3-4</sup> NPR-A is the cognate receptor for atrial natriuretic peptide (ANP) and brain natriuretic peptide (BNP), cardiac-derived hormones that have been well characterised to regulate cardiovascular homeostasis. NPR-C is also a transmembrane protein, however unlike NPR-A and NPR-B it lacks the guanylyl cyclase domain, instead it is a G-protein coupled receptor which modulates adenylyl cyclase, phospholipase C $\beta$  and G-protein-coupled inwardly rectifying potassium channels, the latter of which produces vascular smooth muscle relaxation.<sup>5-6</sup> In addition to this activity NPR-C also mediates a variety of other cardioprotective effects including anti-platelet, anti-leukocyte, anti-hyperthrombotic and antithrombotic activity.<sup>7</sup> NPR-C has received significantly less attention than either NPR-A or NPR-B, in part as this receptor was initially classified simply as a clearance receptor.<sup>8</sup> However, recent studies have demonstrated that NPR-C has defined biological functions including a critical role in the

regulation and maintenance of cardiovascular homeostasis, loss of this signalling is associated with hypertension, cardiac hypertrophy/fibrosis, increased atheroma formation and aneurysm in mouse models.<sup>7,9-10</sup> As such the natriuretic peptide receptors are potentially a new therapeutic target to treat cardiovascular diseases.

The natriuretic peptides ANP, BNP and CNP (**2-4**) are the natural ligands for the NPR receptors and bind with varying specificity to the different receptor types (Figure 1).<sup>11</sup> Several synthetic peptides that bind to these receptors have been developed, such as TAK-639 for NPR-B,<sup>12</sup> the truncated natriuretic peptide cANF<sup>4-23</sup> (**5**)<sup>8</sup> and the agonist PL-3994 (**7**) which are a selective NPR-C agonist and NPR-A agonists respectively.<sup>13</sup> A chimeric peptide approach has also yielded some success, producing the chimeric CD-NP (**6**), a fusion of the active CNP and part of the *Dendroapsis* natriuretic peptide, with an improved *in vivo* profile compared to the natural ligands.<sup>14</sup>

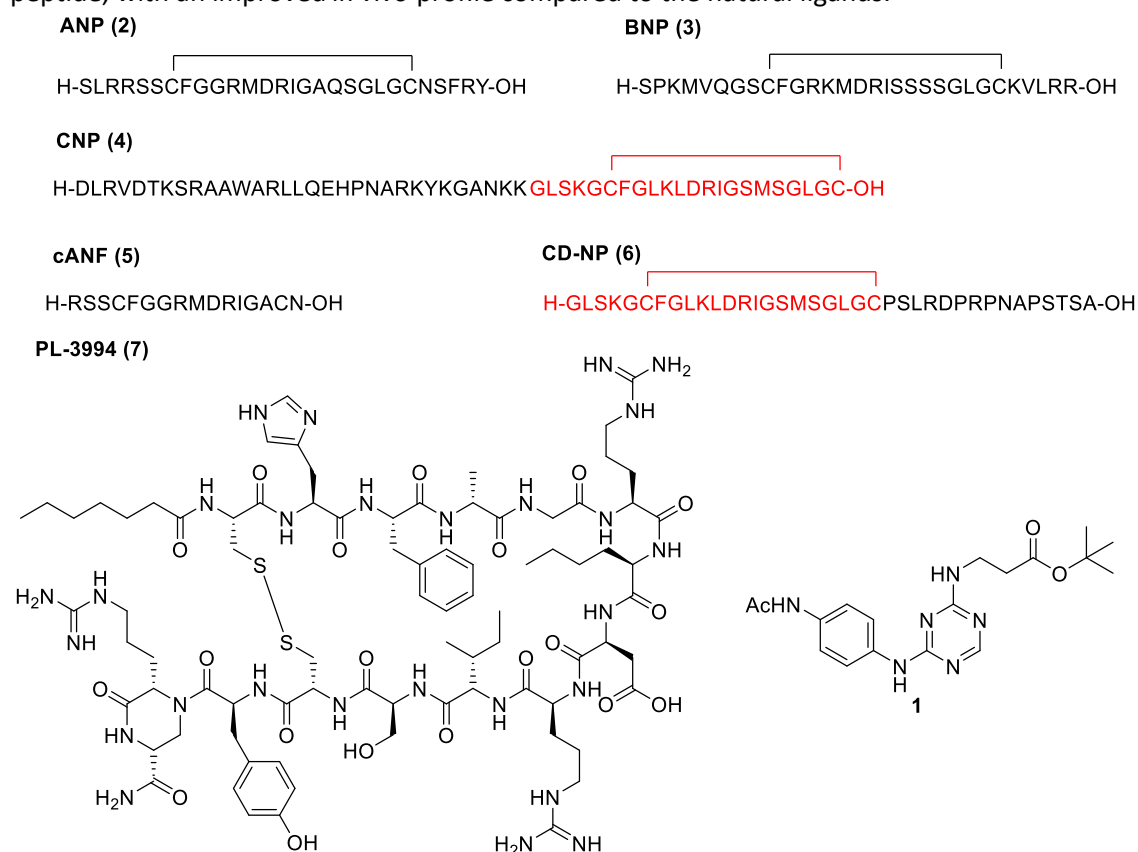


Figure 1. Structures of NPR-C active peptides, and lead compound **1**; active CNP peptide displayed in red, brackets denote disulphide bonds.

Peptidomimetic small molecules that exhibit binding to the natriuretic peptides have been developed, such as the antagonist M372049 (**8**, Figure 2).<sup>15-16</sup>

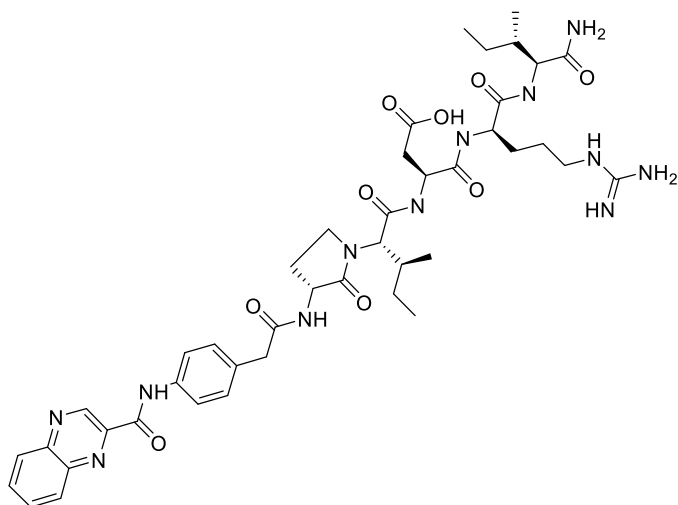


Figure 2. Peptidomimetic ligand active against NPR-C.

In 2008 a series of triazine-based compounds acting as NPR-A agonists were disclosed in a patent (**9-10**, Figure 3),<sup>17</sup> and in 2017 a series of three papers expanded upon this work and disclosed a second series of NPR-A agonists with selectivity optimised for human and rat NPR-A, with *in vitro* and *in vivo* activity (**11-12**), however the method of NPR-A activation was not disclosed in these publications and no binding data of these compounds for NPR-A or the other NPR's was provided.<sup>18-20</sup> We recently reported a small series of NPR-C agonists with low micromolar potency in *in vitro* and *in vivo* models, exemplified by the lead compound **13** depicted in Figure 3.<sup>7</sup>

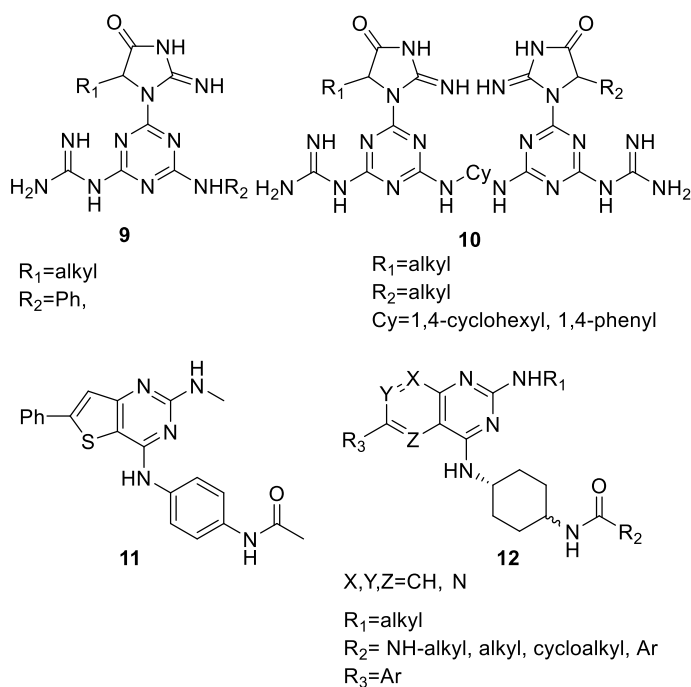


Figure 3. Small Molecule NPR-A and NPR-C agonists

We are interested in the potential of NPRC agonists as potential treatments for heart failure and myocardial infarction. A small molecule agonist would be an ideal drug candidate as an alternative to the natural cyclic peptide ligands, which have significant challenges in both production and delivery to achieve a clinical effect.

Herein we report the development of a series of new series of small molecule agonists for the NPR-C receptor. A detailed study of the structure activity relationships (SAR) and evaluation of pharmacokinetic parameters of key compounds was undertaken, which allowed identification of **1** with potent *in vitro* biological activity and promising *in vitro* and *in vivo* DMPK data.

## Results and discussion

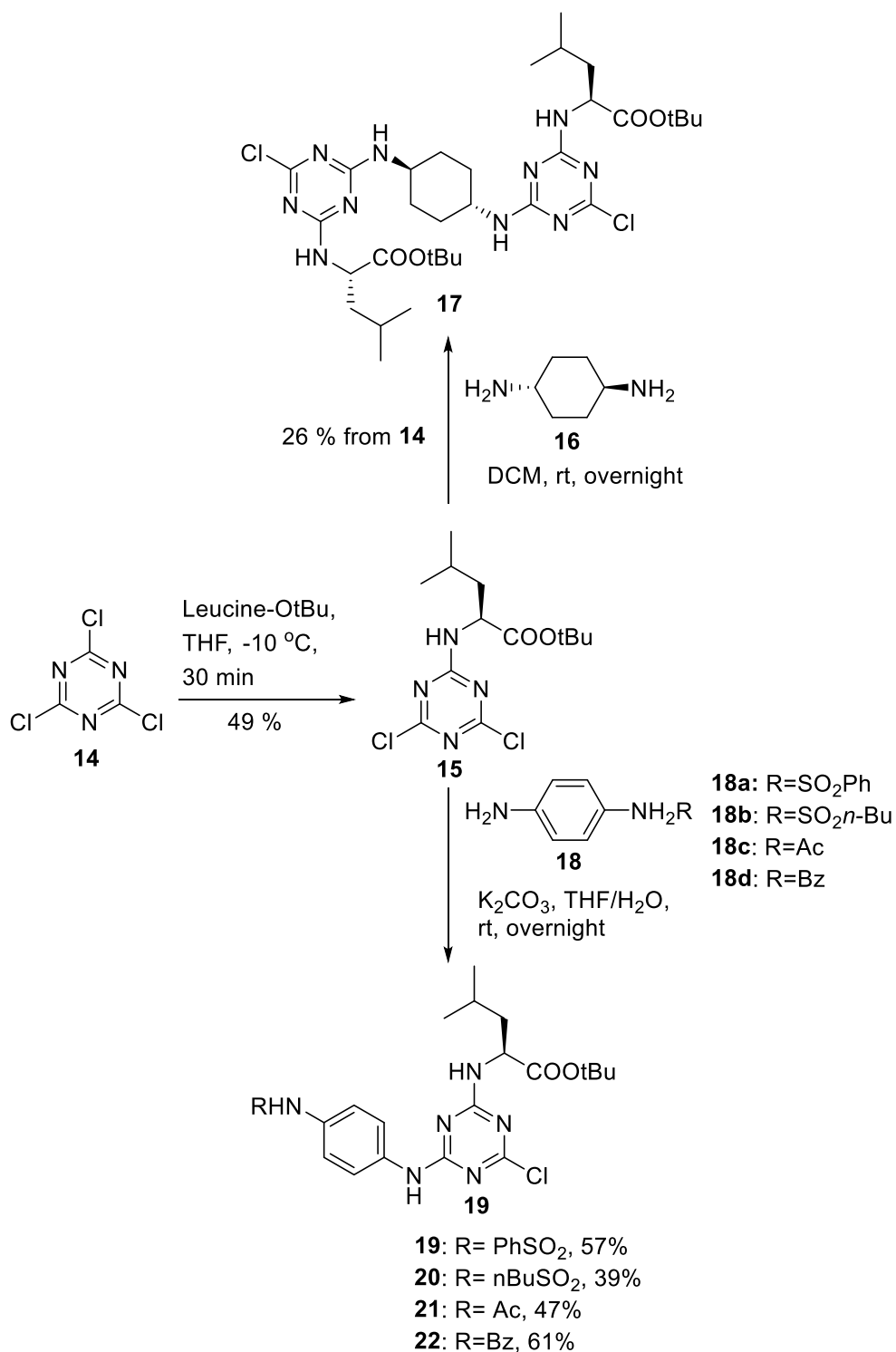
### Design of NRPC agonists

A patent filed in 2008 reported several triazine-based scaffolds (Figure 3) capable of NPR-A agonism;<sup>17</sup> given that the NPR-A and NPR-C receptors bind the same natural ligands and there was no reported selectivity data for these scaffolds, the core motifs were considered a potential starting point for development of a series of NPR-C agonists. The reported molecules were notably non-drug like and in the first instance we opted to both simplify the synthesis and probe structure-activity relationships. It was decided not to install the guanidino functionalities, but to leave the acyclic amino acid group, which was a successful motif in the previous small molecule agonists prepared.<sup>7</sup>

### Chemistry

Synthesis of the initial series of analogues proceeded by adapting established chemistry for substitution of chlorotriazine derivatives,<sup>19</sup> treatment of 1,3,5-trichlorotriazine (**14**) with the *tert*-butyl ester of leucine at -10°C in THF formed the nucleophilic aromatic substitution adduct **15** which underwent dimerization with *trans*-1,4-diaminocyclohexane in a one-pot process to provide **17** (Scheme 1). Several truncated analogues **19-22** were also prepared from **14** in two steps and in moderate yields by treatment of **15** with potassium carbonate in a mixture of THF/water with the *p*-phenylenediamine-derived subunits (**18a-d**) with different capping groups to probe whether

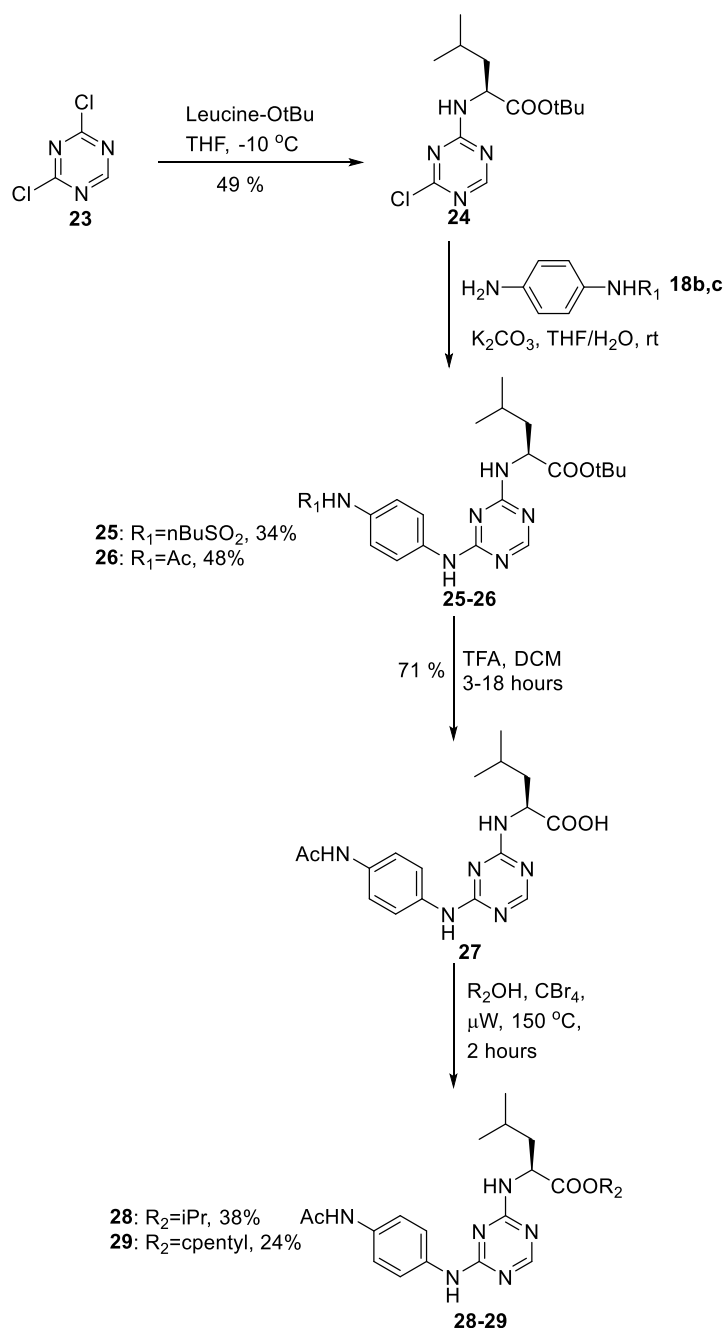
dimerization was necessary. The moderate yields were consistent with those previously obtained in the literature for similar transformations.<sup>19</sup>



Scheme 1. Synthesis of 1,4-cyclohexane disubstituted bis-triazine and monomeric chlorotriazine derivatives.

Further analogues of **19** without the additional chlorine atom were prepared from dichlorotriazine (**23**) by sequential nucleophilic aromatic substitution with leucine tert-butyl ester and substituted phenylene diamine subunits to afford **25-26** in moderate yields using the methods previously

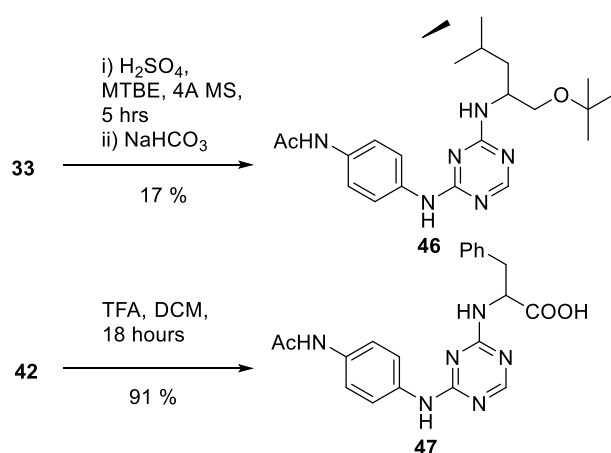
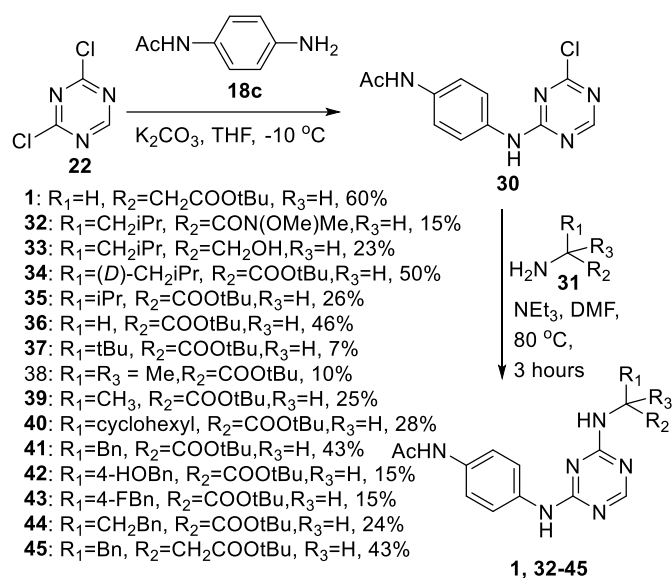
described (Scheme 2). Yields compared favourably to similar transformations in the literature, which show significant variance, particularly for the second substitution step (from 5 % to >95 %), although sulfoxide and sulphonamide derivatives were typically associated with lower yields.<sup>21-28</sup> Removal of the *t*-butyl ester was performed under standard acid hydrolysis reaction conditions to provide **27**,<sup>29</sup> and a series of ester derivatives were prepared using procedures adapted from the literature to afford **28-29** in moderate yields.<sup>30</sup>



Scheme 2. Synthesis of L-valine triazine derivatives

The synthesis of derivatives with different amino acids followed the previously established chemistry, starting from 2,3-dichlorotriazine (**20**) the common intermediate **30** was prepared through nucleophilic aromatic substitution (Scheme 3). A second nucleophilic aromatic substitution

was performed at elevated temperatures in order to shorten the reaction time (3hat 80°C cf. overnight at room temperature) to afford **1, 32-45** in low to moderate yields. Lower yields were typically obtained for molecules with complex functionality (e.g. free OH; **33, 42**, labile amide; **32**) and shorter, sterically demanding side chains (**35, 37, 38, 40**), for the former stability issues could explain the lowered yields. Alkylation of **33** using a SN1 type substitution afforded the t-butyl ether **46** in 17 % yield and acid promoted hydrolysis of **41** provided the phenylalanine acid derivative **47** in high yield.



Scheme 3. Synthesis of amino acid substituted triazines.

### Biological evaluation

At the outset of this study, we faced the challenge of how to assemble meaningful structure activity relationships with only a low-throughput functional pharmacological assay in isolated blood vessels available for determination of agonism. To address this issue we developed two orthogonal binding assays for NPR-C using the extracellular domains of the receptor, a surface plasmon resonance assay using conventional amide coupling of the protein to a dextran coated chip, and a fluorescence polarization assay based on displacement of a fluorescent NPR-C binding peptide, this work has been reported elsewhere.<sup>31</sup> While binding is not necessarily related to agonism "*Corpora non agunt nisi fixate*" it allowed us to triage the compounds for affinity and active site occupancy, and then to follow up with detailed organ bath studies for agonism.

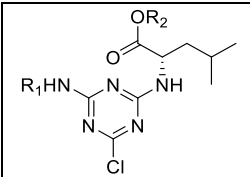
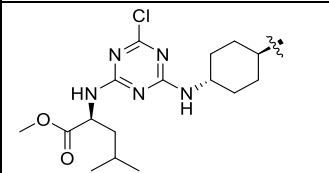
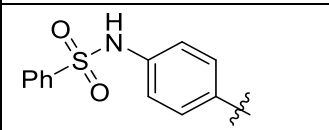
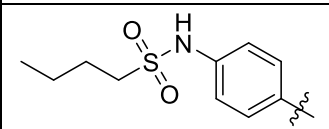
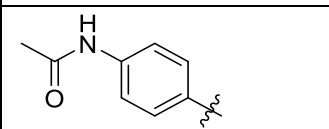
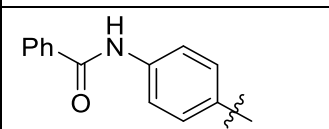
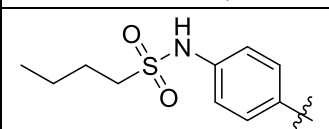


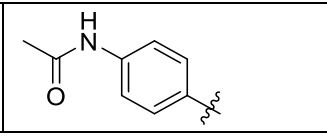
## Binding evaluation using surface plasmon resonance.

Binding of these compounds to NPR-C was evaluated by surface plasmon resonance (SPR), in the first instance a binding analysis is used to validate analyte binding, whereupon a full kinetic-affinity assay is performed to calculate accurate  $K_D$  values using the affinity method. Molecules which displayed a very low response (<20% at 60  $\mu\text{M}$ ) in the binding assay and those with a  $R_{\text{max}}$  value much greater than the theoretical maximum were not taken on for further testing, as these are signs of non-specific/weak binding.

Analysis of the SPR data revealed that **17** bound with moderate  $K_D$  of  $95.7 \pm 1.7 \mu\text{M}$  (Table 1). The binding of the truncated analogues compared favourably to this, with **19** binding with a similar  $K_D$  value of  $99 \pm 52 \mu\text{M}$ , whilst the alkylthioamide and acetamide-capped analogues **20** and **21** displayed more potent binding than the dimeric **17**, with  $K_D$  values of  $25.7 \pm 6.9$  and  $36.9 \pm 1.6 \mu\text{M}$  respectively. The benzamide derivative **22** displayed a poor binding profile in the initial SPR screen and was not taken on for full characterisation. The *des*-chloro analogues **25** and **26** of the monomeric compounds were found to bind with a similar level of potency ( $K_D$   $45.1 \pm 1.9 \mu\text{M}$  and  $30.8 \pm 1.3 \mu\text{M}$  respectively) to the chlorinated derivatives. Compound **26** with the acetamide capping group was selected as a potential lead compound for further development and analysis of structure activity relationships.

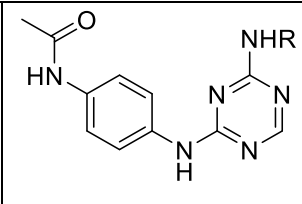
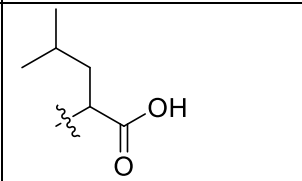
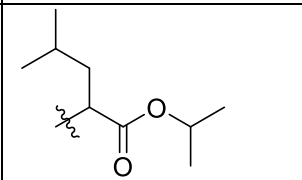
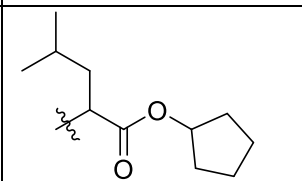
Table 1. The effect of changes to the aryl and cycloalkyl groups on NPR-C binding.

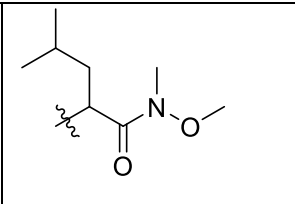
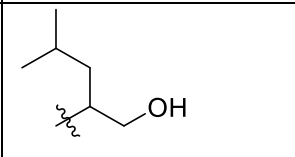
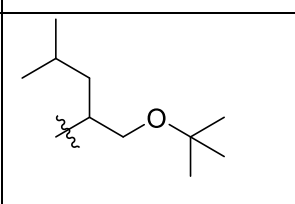
	R <sub>1</sub>	R <sub>2</sub>	$K_D$ ( $\mu\text{M}$ ) <sup>a</sup>
<b>17</b>		CH <sub>3</sub>	$95.7 \pm 1.7$
<b>19</b>		tBu	$99 \pm 52$
<b>20</b>		tBu	$25.7 \pm 6.9$
<b>21</b>		tBu	$36.9 \pm 1.6$
<b>22</b>		tBu	$R_{\text{max}} \gg \text{theoretical}$
<b>25</b>		tBu	$45.1 \pm 1.9$

<b>26</b>		tBu	30.8±1.3
<sup>a</sup> The SPR experiments were repeated with similar results			

Next the effect of the amino acid ester on the SAR was investigated (Table 2). The leucine free acid analogue **27** resulted in significantly reduced potency in the SPR experiment, with a  $K_D$  of 220.4±22.6  $\mu\text{M}$ . The isopropyl ester analogue **28** likewise displayed less potent binding ( $K_D$  84.4±2.8  $\mu\text{M}$ ), interestingly the cyclopentyl ester **29** retained the binding potency ( $k_D$  25.0±3.1  $\mu\text{M}$ ) with a slight improvement over **26**. Removal of the ester carbonyl to furnish the t-butyl ether analogue **46** maintained comparable binding potency ( $K_D$  42.2±9.6  $\mu\text{M}$ ); whilst the alcohol analogue **33** suffered a significant reduction in potency ( $KD$  163.6±6.1  $\mu\text{M}$ ), which indicated that the non-polar functionality was more important than possible hydrogen bonding interactions of the carbonyl. The Weinreb amide **32** likewise reduced the potency of binding with a  $K_D$  of 144.3±7.7  $\mu\text{M}$ . This information would suggest the ester group is located near a nonpolar binding pocket, and that the ester carbonyl may be involved in a minor stabilising interaction (H-bonding) which is lost upon reduction of the carbonyl to the alcohol or ether. Whilst the cyclopentyl ester **29** has slightly increased potency compared to the t-butyl ester of **26**, given the commercial availability of precursors and shorter synthetic route, the t-butyl ester motif was retained for future analogues.

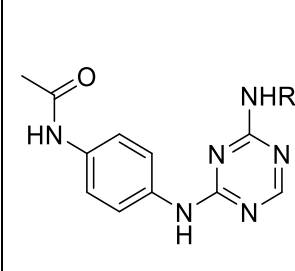
Table 2. Exploration of binding affinity with variations to the ester group.

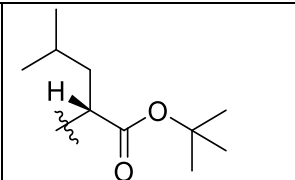
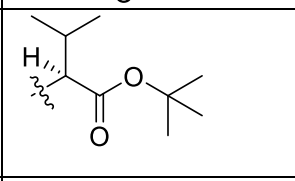
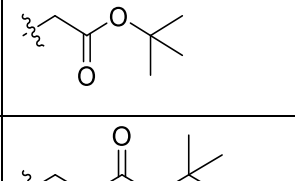
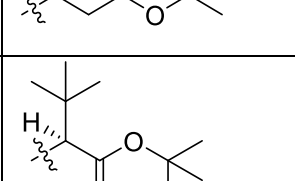
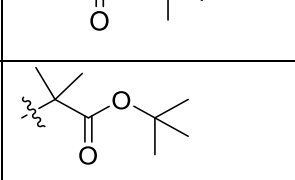
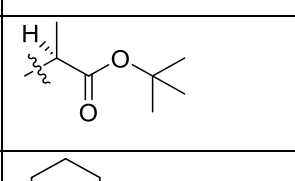
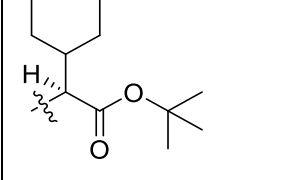
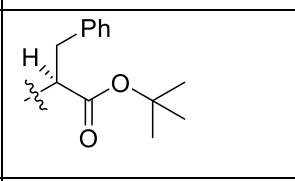
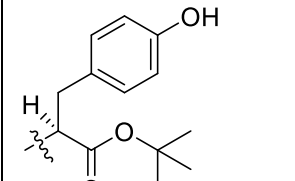
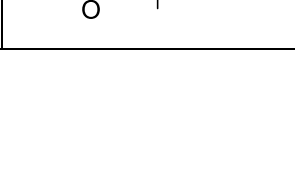
		$K_D$ ( $\mu\text{M}$ ) <sup>a</sup>
	R	
<b>27</b>		220±22
<b>28</b>		84.4±2.8
<b>29</b>		25.0±3.1

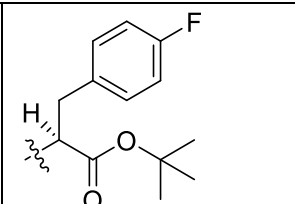
<b>32</b>		144.3±7.7
<b>33</b>		163.6±6.1
<b>46</b>		42.2±9.6
<sup>a</sup> The SPR experiments were repeated with similar results.		

With SAR around the ester in hand it was desired to examine the effect of the amino acid R group (Table 3). In order to determine the optimal geometry at the stereocentre the D-leucine derivative **34** was prepared and had reduced potency compared to the lead **26**, failing to pass the preliminary binding screen for full SPR analysis. The valine analogue **35** with a shorter isopropyl side chain also resulted in a decreased binding potency in the SPR assay ( $K_D$  79±47µM). The glycine (**36**), β-alanine (**1**) and *t*-butyl (**37**) derivatives displayed a loss of binding potency with  $K_D$  values over 100 µM. The dimethylalanine and alanine analogues **38-39** did not meet the minimum binding threshold to receive full SPR analysis. From these results larger and smaller acyclic aliphatic chains and no side chain were found to be detrimental to binding activity. In contrast, cyclic aliphatic sidechains such as that in **40** retained the binding potency compared to **26**, with a  $K_D$  of 28.0±4.9 µM. The phenylalanine analogue **41** retained the binding potency of the lead compound **26** with a  $K_D$  31.3±7.3 µM, whilst the electron deficient 4-fluorophenylalanine analogue **43** had a slight increase in potency,  $K_D$  23.73±3.8 µM. It should be noted that the tyrosine analogue **42** did not meet the minimum binding threshold for full SPR analysis.

Table 3. Exploration of binding affinity for different amino acid analogues.

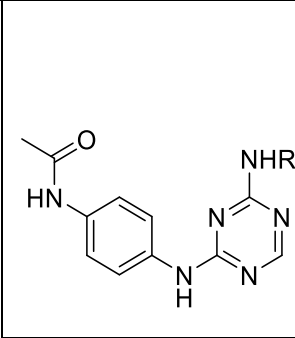
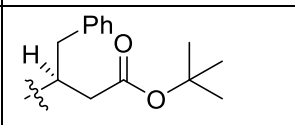
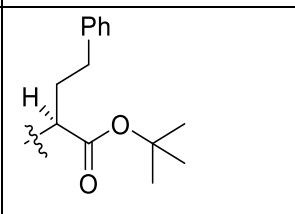
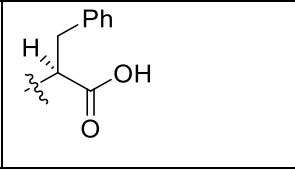
		$K_D$ (µM) <sup>a</sup>
	R	

34		Rmax<20%
35		79±47
36		832±190
1		146±39
37		201.3±6.1
38		Rmax<20%
39		Rmax<20%
40		28.0±4.9
41		31.3±7.3
42		Rmax<20%

<b>43</b>		23.7±3.8
<sup>a</sup> The SPR experiments were repeated with similar results		

Further exploration of the phenylalanine analogue SARs was warranted due to potent binding in the SPR assay (Table 4. Exploration of phenylalanine SAR.), to this end the effect of chain extensions of both the ester and benzyl portion of the molecule, analogues **44** and **45** respectively was examined; the former retained binding potency of the parent compound ( $K_D$  29.60±4.5  $\mu$ M), whilst the latter had slightly increased potency with a  $K_D$  of 23.8±2.0  $\mu$ M. The free acid analogue **47** did not have a detectable change in binding potency ( $K_D$  38±17  $\mu$ M) compared to **41**, however this is an improvement over the valine free acid analogue **27**, which suffered a substantial decrease in potency compared to the lead *t*-butyl analogue **26**.

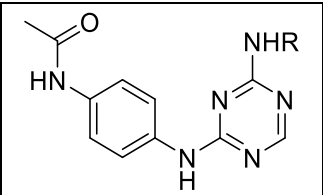
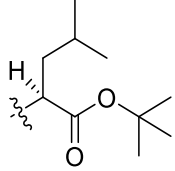
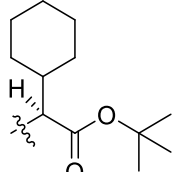
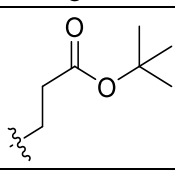
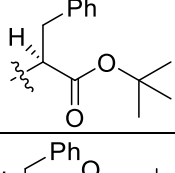
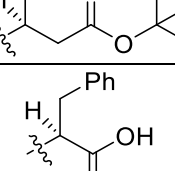
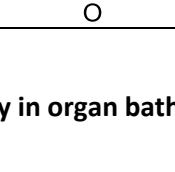
Table 4. Exploration of phenylalanine SAR.

		$K_D$ ( $\mu$ M) <sup>a</sup>
		
	R	
<b>44</b>		29.6±4.5
<b>45</b>		23.8±2.0
<b>47</b>		38±17
<sup>a</sup> The SPR experiments were repeated with similar results.		

### Exploration of competitive binding to NPR-C using fluorescence polarization.

We previously developed a fluorescence polarization assay for the NPR-C extracellular domains.<sup>31</sup> This allowed us to determine if our compounds displaced a fluorescently labelled agonist peptide from the agonist binding region. Selected analogues were evaluated in this assay (Table 5). Analogues **26** and **44** were inactive in this assay, and **40** displayed a substantially lower response in this assay compared to the SPR result. In a primary screen for binding activity the analogue **1** displayed minimal activity in this assay with low binding (<17%) at 300  $\mu$ M, and was not subjected to a full concentration-response assay as a result. Analogues **41** and **47** displayed comparable potency to the SPR assay. Whilst the competition data does not mirror the SPR results, it indicates that molecules from this series act on the NPR-C receptor at the same site as the peptide agonists.

Table 5. Competitive binding of selected NPR-C agonists.

	R	FP EC <sub>50</sub> ( $\mu$ M)	SPR K <sub>d</sub> ( $\mu$ M)
<b>26</b>		Inactive	30.8 $\pm$ 1.9
<b>40</b>		326.7 $\pm$ 12.3	28.0 $\pm$ 4.9
<b>1</b>		Low % binding	146 $\pm$ 39
<b>41</b>		32 $\pm$ 15	31.3 $\pm$ 7.3
<b>44</b>		Inactive	29.6 $\pm$ 4.5
<b>47</b>		60 $\pm$ 10	38 $\pm$ 17

### NPR-C agonist activity and selectivity in organ bath studies

The vasodilatory effect of promising molecules as identified from SPR and competitive binding data was evaluated against both mouse small mesenteric artery (SMA) and rat aorta models (Table 6). When run with appropriate controls and challenged with specific antagonists these assays provide measures of NPR-C agonist activity in separate rodent species, at the time of writing there is no published data showing NPR-C causes vasorelaxation in the rat aorta.<sup>7</sup> Dimeric compound **17** displayed low micromolar EC<sub>50</sub> values, in both mouse SMA (0.97 ± 1.17 μM) and rat aorta (1.43 ± 3.06 μM). Analogues **27**, **39**, **40** and **43** displayed a less potent response in these tissues, with a higher potency generally observed in the mouse SMA, although a notable exception to this is the acid analogue **27** which displayed a higher potency in the rat aorta. β-alanine analogue **1** displayed sub-micromolar activity in rat SMA (0.86±0.23 μM) but was less potent in the rat aorta (17.11 ± 68.07 μM). Phenylalanine analogue **41** retained potency (0.39 ± 0.08 μM) in the mouse SMA, however, was substantially less potent in the rat aorta (>100 μM). Interestingly, the chain-extended phenylalanine analogues **44** and **45** had improved potency (21.38 ± 11.00 μM and 3.76 ± 2.24 μM respectively) in the rat aorta relative to **41** (>100 μM). The structure-activity relationships derived from the SPR data largely hold true for these biological assays, with larger, non-polar R-groups and ester's eliciting a more potent response. However, there was a significant difference in potency between the mouse SMA and rat aorta, for most compounds tested (up to three orders of magnitude difference), which could not be fully accounted for.

The selectivity of these molecules to target NPR-C was also examined for several compounds using both mouse SMA treated with a selective NPR-C antagonist (M372049 or osteocrin) and by comparison of SMA from wild-type and NPR-C knockout (KO) animals to validate that the observed biological effect could be contributed to NPR-C agonism. Each of the compounds tested displayed a significant rightward-shift in their concentration response relationship in the presence of NPR-C antagonist or in NPR-C KO tissue, although this was not a complete inhibition of vasodilation. For example, the positive control cANF<sup>4-23</sup> effectively displayed a complete loss of potency (Figure 4A), whilst **1** showed between 2.5 and 10 fold reduction in potency (EC<sub>50</sub> value) when treated with osteocrin or M372049 respectively (Figure 4B), which was consistent with a loss of NPR-C signalling.

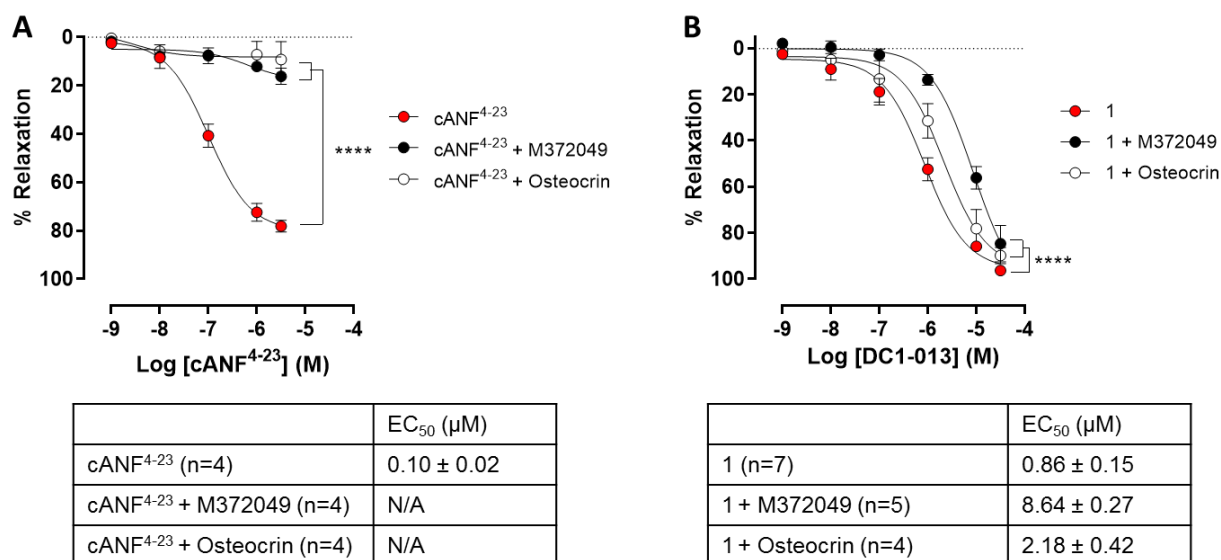
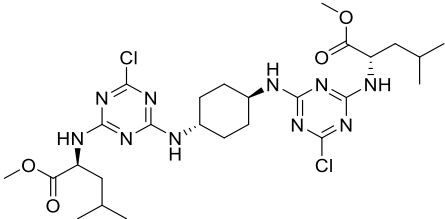
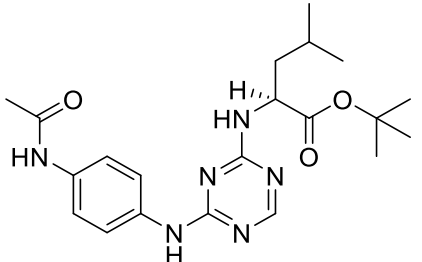
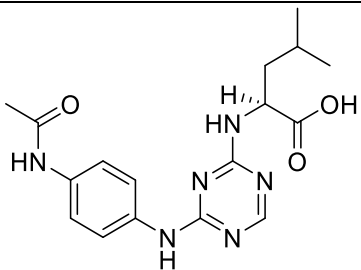


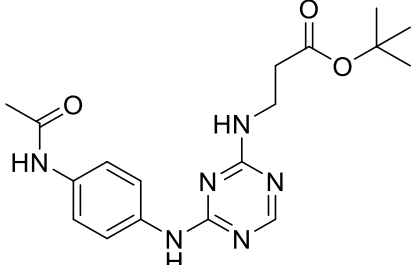
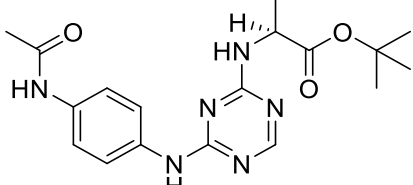
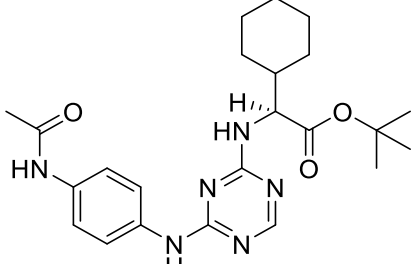
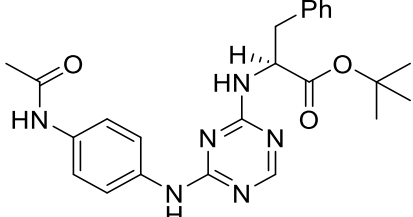
Figure 4. Reversal of agonist induced vasorelaxation upon treatment with NPR-C inhibitors in rat small mesenteric artery. **A** The selective NPR-C peptide agonist cANF<sup>4-23</sup> causes vasorelaxation that is blocked by M372049 and osteocrin; **B** small molecule agonist **1** causes vasorelaxation that is partially blocked by M372049 and osteocrin.

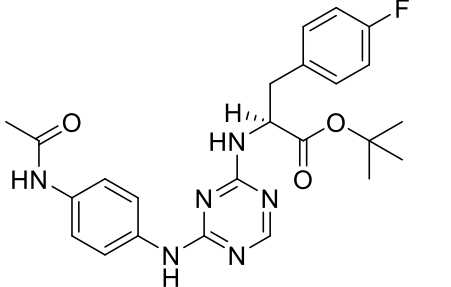
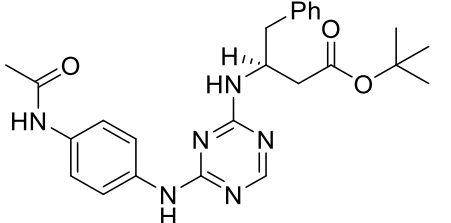
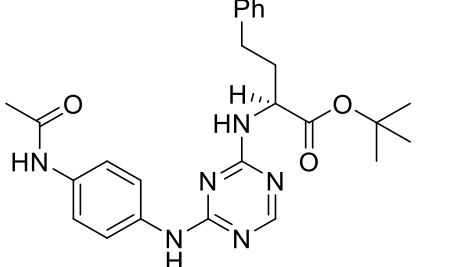
The dimer **17** displayed mixed results in these assays, with an increase in potency when applied to SMA treated with NPR-C antagonist M372049 ( $0.47 \pm 0.68$  cf.  $0.97 \pm 1.17$   $\mu\text{M}$ ), with a decrease in potency observed in the KO SMA ( $2.64 \pm 1.10$  cf.  $1.25$   $\mu\text{M}$ ). This mixed result would require further investigation to confirm involvement of NPR-C in this molecule's biological activity. Phenylalanine analogue **41** displayed no significant change in potency in either assay, which calls into question the cause of vasodilation for this analogue. These results indicate that whilst a portion of the biological activity is caused by NPR-C signalling, there is also some off-target activity contributing to the observed vasodilation, which complicated further optimisation of structure-activity relationships from this data. Other functional assays to assess NPR-C activation (e.g. cAMP production, *vide infra*) were unaffected by the inherent vasorelaxation caused by these molecules.



Table 6. NPR-C Agonist evaluation in small mesenteric artery and rat aorta.

	Compound	Rat small mesenteric artery		Rat aorta	Mouse small mesenteric artery	
		EC <sub>50</sub> (μM)	EC <sub>50</sub> +NPR-C inhibitor (M372049) (μM)	EC <sub>50</sub> (μM)	WT EC <sub>50</sub> (μM)	NPR-C KO EC <sub>50</sub> (μM)
<b>17</b>		0.97 ± 1.17 (n=4)	0.47 ± 0.68 (n=3)	1.43 ± 3.06 (n=4)	1.25 (n=1)	2.64 ± 1.10 (n=3)
<b>26</b>		0.30 ± 0.31 (n=5)	1.18 ± 1.00 (n=3)	0.53 ± 0.73 (n=4)	0.55 ± 0.17 (n=2)	0.85 ± 0.55 (n=4)
<b>27</b>		22.18 ± 34.61 (n=3)	n.t.	6.20 ± 9.72 (n=3)	n.t.	n.t.

1		$0.86 \pm 0.23$ (n=7)	$8.64 \pm 1.96$ (n=5)	$17.11 \pm 68.07$ (n=6)	$1.11 \pm 0.85$ (n=2)	$10.09 \pm 12.9$ (n=4)
39		$3.45 \pm 6.33$ (n=3)	n.t.	$78.07 \pm 0.00$ (n=2)	n.t.	n.t.
40		n.t.	n.t.	$6.24 \pm 12.87$ (n=4)	n.t.	n.t.
41		$0.39 \pm 0.08$ (n=5)	$0.36 \pm 0.07$ (n=3)	$102.2 \pm 1.80$ (n=5)	$3.20 \pm 7.03$ (n=2)	$3.02 \pm 0.51$ (n=4)

43		n.t.	n.t.	4.43 ± 2.36 (n=4)	n.t.	n.t.
44		n.t.	n.t.	21.38 ± 11.00 (n=2)	n.t.	n.t.
45		n.t.	n.t.	3.76 ± 2.24 (n=4)	n.t.	n.t.

### Human NPR-C evaluation in HeLa cells.

Human HeLa cells express a functional NPR-C receptor and represent a useful direct way to determine NPR-C agonist activity through the measurement of an agonist induced decrease of downstream cAMP levels.<sup>6</sup> We evaluated **1** in this model and compared the response with the selective NPR-C agonist cANF<sup>4-23</sup>. cANF<sup>4-23</sup> caused a clear decrease in the cAMP levels induced with the adenylyl cyclase stimulator forskolin and this was reversed by the antagonists M372049 and osteocrin (Figure 5A). A similar reduction of cAMP was induced upon the addition of **1** and this was reversed by antagonist application (Figure 5B).

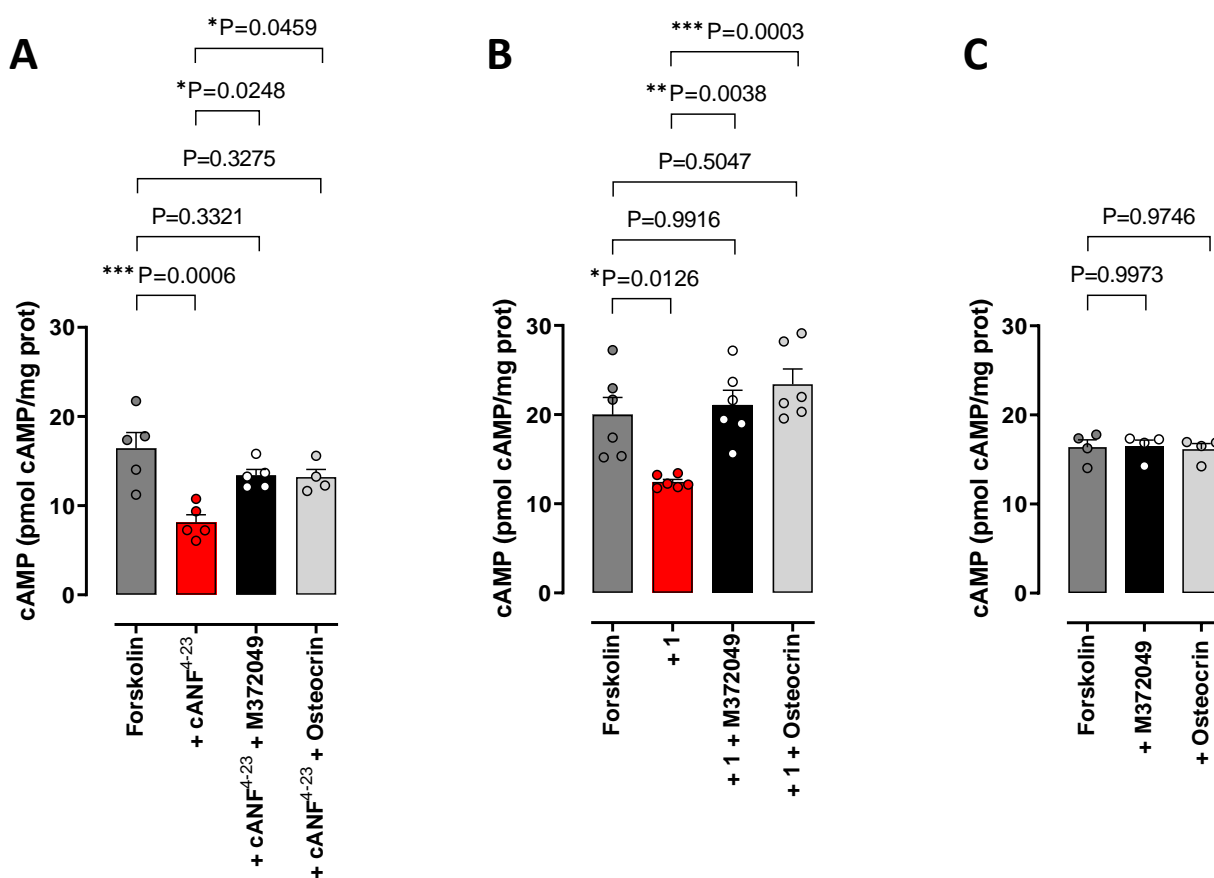


Figure 5. Evaluation of NPR-C agonism in HeLa cells by a cAMP assay. **A** cANF<sup>4-23</sup> inhibits cAMP formation that is reversed by M372049 and osteocrin; **B** small molecule agonist **1** modestly inhibits cAMP formation that is reversed by M372049 and osteocrin; **C** M372049 and osteocrin do not affect basal forskolin-induced cAMP production.

### ADME data

Several promising analogues with diverse structures were evaluated for ADME properties, the data is presented in (Table 7). Solubility and membrane permeability assessed by PAMPA predictably displayed an inverse correlation, with the dimeric **17**, free acid **27** and glycine derivative **36** lacking a

non-polar R group displayed relatively high solubility of >70 mg/mL, and low membrane permeability ( $<1 \times 10^{-6}$  cm/s) whilst the more non-polar **26** and **41** were almost insoluble (0.414, 11.61 mg/mL), but have improved membrane permeability (6.07 and  $7.35 \times 10^{-6}$  cm/s respectively). The dimer **17** displayed long half-life in rat hepatocytes (>200 min) which was also evident in human plasma (>60 min). However, in both rat and human plasma was almost completely bound to plasma protein (>99.5%) and two CypP450 isoforms were inhibited ( $EC_{50}$  4.96-37.8  $\mu$ M). The more lipophilic **26** had high clearance rate and consequently low half-life in rat hepatocytes (12 min), but retained the long half-life in human plasma. There was also inhibition of a half dozen CypP450 isoforms ( $EC_{50}$  7.30-30.6  $\mu$ M). Phenylalanine analogue **41** suffers from similar issues with long half-life in human plasma (>120 min) but a high proportion (97.2 %) bound to plasma proteins and a high clearance rate and consequently low half-life in rat hepatocytes and plasma (<10 minutes). Additionally, there was potentially problematic inhibition of five CypP450 isoforms ( $EC_{50}$  7.72-19.8  $\mu$ M). The  $\beta$ -alanine derivative **1** (DC1-013) displayed more favourable properties, with decreased clearance and increased half-life in rat hepatocytes with a half-life of almost two hours, long half-life (>120 minutes) in human plasma, lower binding to plasma proteins (71 %) and all CypP450 isoforms tested had inhibition  $EC_{50}$  >50  $\mu$ M. The free acid valine analogue **27**, which substantially improves the pharmacokinetic properties compared to the *t*-butyl ester **26**, had a half-life in rat hepatocytes of over three hours and >60 minutes half-life in human plasma, with only 85% bound to plasma proteins and high  $EC_{50}$  (>50  $\mu$ M) for all CypP450 isoforms tested.

The lipophilic analogues **26** and **41** with the highest potency in both SPR and biological assays performed the worst in terms of pharmacokinetic profiles, with the more polar analogues providing a better pharmacokinetic profile. Promisingly the leucine free acid analogue **27** did not have the clearance or CypP450 inhibition issues of the *t*-butylester. Whilst this analogue was substantially less potent than the *t*-butylester, the phenylalanine free acid analogue **47** retained potency in the SPR assays and would be expected to follow the same pharmacokinetic trends displayed by the leucine analogues.

With this data in hand **1** was selected for an *in vivo* bioavailability study and the results are shown (Table 8Table and Table 9). **1** displayed a promising profile with low clearance of 112 mL/min/kg and >40% bioavailability.

Table 7. Solubility, permeability and In vitro metabolism.

compound	Solubility (mg/mL)	PAMPA P <sub>app</sub> (cm/Sx10 <sup>-6</sup> )	Hepatocyte (rat)		Human Plasma T <sub>1/2</sub> (min)	Plasma Protein binding (% bound)	Cyp P450 inhibition (IC <sub>50</sub> μM)
			T <sub>1/2</sub> (min)	CL (μL/min/10 <sup>6</sup> )			
<b>17</b>	>122.52	<0.023	>216.8	<0.64	>60	99.5	2C9 (4.96) 2C19 (37.8)
<b>26</b>	<0.414	6.07	12.2	113.7	>120	94.1	1A2 (26.8) 2C8 (7.30) 2C9 (30.6) 2C19 (16.4) 3A4-M (29.9) 3A4-T (16.7)
<b>41</b>	11.61	7.35	6.0	230.4	>120	97.2	2C8 (7.72) 2C9 (17.7) 2C19 (14.7) 3A4-M (19.8) 3A4-T (11.6)
<b>1</b>	71.71	0.94	117.9	11.8	>120	71.0	All>50
<b>27</b>	>71.68	<0.001	216.8	<6.4	>60	85.4	All>50

Table 8. Intravenous PK profile of **1** after dosing at 3mg/kg (mice).

PK Parameters	Mean	SD
	IV	
$C_0$ (ng/mL)	2328 ±	233
$T_{1/2}$ (h)	0.566 ±	0.293
$Vd_{ss}$ (L/kg)	1.75 ±	0.121
Cl (mL/min/kg)	112 ±	10.1
$AUC_{0-inf}$ (ng.h/mL)	448 ±	42.3
$MRT_{0-inf}$ (h)	0.262 ±	0.0377

Table 9. Oral PK profile of **1** after dosing at 10mg/kg (mice).

PK Parameters	Mean	SD
	PO	
$C_{max}$ (ng/mL)	612 ±	139
$T_{max}$ (h)	0.250 ±	0.000
$T_{1/2}$ (h)	1.37 ±	0.567
$AUC_{0-inf}$ (ng.h/mL)	653 ±	141
$MRT_{0-inf}$ (h)	1.33 ±	0.209
Bioavailability (%) <sup>a</sup>	43.8 ±	--

## Conclusion

We have designed and synthesised a series of NPR-C agonists based upon molecules reported to bind the related natriuretic peptide receptor A. These compounds were tested in several assays in order to establish structure activity relationships which identified several compounds as binding to the target receptor. The link between receptor binding and biological effect was confirmed by vasodilation assays carried out on SMA and rat aorta, **26** and **41** were found to be potent at a sub-micromolar level. However, control experiments revealed some off-target activity. This off-target activity might be the result of NPR-A or NPR-B agonism, and further assays (i.e. cGMP measurement) would be required to assess this (i.e. an index of NPR selectivity). Nevertheless, the loss of activity in cell-based assays in the presence of M372049 and/or osteocrin suggests robust target engagement.<sup>11, 15-16</sup> One molecule **1** showed selective NPR-C agonism in humans, mice and rats, and demonstrated a promising pharmacokinetic profile.

## Experimental

### Materials and Methods

Commercially available starting materials were used as supplied without further purification. Reactions were carried out in dry solvents (DCM, DMF, THF, cyclobutanol, cyclopentanol, isopropanol) unless otherwise noted. Reactions were monitored by thin layer chromatography (TLC) and Agilent 6100 single quadrupole LC 1200 series mass spectrometer. Purification was carried out on either a Biotage Isolera one or Biotage Isolera four system, with either C18 or Silica gel prepacked columns. <sup>1</sup>H and <sup>13</sup>C NMR data were recorded on a 600 MHz Bruker Avance III with a 5mm helium-cooled cryoprobe. Chemical shifts for <sup>1</sup>H and <sup>13</sup>C spectra were referenced to residual solvent. Mass spectra were obtained on an Agilent 1200 liquid chromatograph system connected to an Agilent 6100 single quadrupole mass spectrometer. HRMS-ESI data were obtained on an Agilent 1200 liquid chromatograph system connected to Agilent 6510 QTOF mass spectrometer. Purity was determined by LCMS analysis and is >95% for all compounds unless otherwise stated.

Human full-length (FL) NPR-C (27–541)-10His-Flag (GenBank accession: NM\_000908) and extracellular domain (ECD) NPR-C (27–481)-6His were purchased from Peak Proteins, UK. The FP probe 5-carboxyfluorescein N-terminus labelled GLSKG[CFGRSLDRIGLSGLGC]NS (P19) was purchased from Peptide Protein Research Ltd, UK (Peptidesynthetics).

### PAINS Statement

All compounds tested in these assays (**1**, **17**, **19**, **20-22**, **25-29**, **32-47**) were run through the computational PAINS checkers <http://zinc15.docking.org/patterns/apps/checker/> and <https://www.cbligand.org/PAINS/login.php>. All structures passed this analysis, no PAINS flags were indicated. In addition, the two assays detailed in Figures 4 and 5 show dose-dependent competitive inhibition of **1** with the known NPR-C antagonist M372049, which provides unambiguous evidence of target engagement.

### Chemistry

**18a-d** were prepared following established literature procedures.<sup>32,33,34</sup>

#### **tert-butyl 3-((4-((4-acetamidophenyl)amino)-1,3,5-triazin-2-yl)amino)propanoate (1)**

To a solution of **30** (100 mg, 0.379 mmol) and t-Bu β-alanine HCl (103 mg, 0.569 mmol) in dry DMF (2 mL) at r.t. was added triethylamine (0.133 mL, 0.948 mmol) and the mixture stirred at 80°C for 3h (TLC, LCMS). To the reaction was then added water, and the resultant solid was filtered, washed with water and then dried. Column chromatography (1:3, c-Hex, EtOAc) afforded the title compound as a white solid (0.085 g, 0.228 mmol, 60%).

<sup>1</sup>H NMR (600 MHz, DMSO-d<sub>6</sub>) δ/ppm: 9.81 (s, 1H), 9.45 (m, 1H), 8.15 (d, 1H, J = 65 Hz), 7.65 (d, 2H, J = 7.7 Hz), 7.49-7.44 (m, 2H), 3.48 (qn, 2H, J = 6.8 Hz), 2.01 (s, 3H), 1.39 (m, 9H).

<sup>13</sup>C NMR (150 MHz, DMSO-d<sub>6</sub>) δ/ppm: 170.6, 167.9, 165.8, 165.5, 164.9, 134.8, 134.1, 120.4, 119.3, 119.2, 79.9, 36.4, 35.1, 34.7, 27.8, 23.9.

LCMS [M+H] Calcd. for: C<sub>18</sub>H<sub>24</sub>N<sub>6</sub>O<sub>3</sub><sup>+</sup> 373.19; measured 373.00.

#### **dimethyl 2,2'-((((1*r*,4*r*)-cyclohexane-1,4-diyl)bis(azanediyl))bis(6-chloro-1,3,5-triazine-4,2-diyl))bis(azanediyl))bis(4-methylpentanoate) (17)**



To L H-Leu-OMe (1.81 g, 10 mmol) and DIPEA (3.7 mL, 2.58 g, 20 mmol) in DCM (10 mL) at 0°C was added cyanuric chloride (1.84 g, 10 mmol) as a solid in small portions and the reaction stirred at 0°C for 30 min. Water (20 mL) was added, reaction stirred for 5 min then the DCM separated and to this was added the trans diaminocyclohexane (0.98 g, 5 mmol) in DCM (5 mL) and the reaction stirred overnight. The crude reaction mixture was purified directly by Flash chromatography (Puriflash SiO<sub>2</sub>, 40g) using DCM/acetone gradient. This gave the product (0.88 g, 1.28 mmol) 26% yield.

<sup>1</sup>H NMR (400 MHz, DMSO, 70° C) δ 7.89 (s, 1H), 7.61 (s, 1H), 4.48 (s, 1H), 4.39 (s, 1H), 3.69 (s, 2H), 3.65 (s, 6H), 1.90 (s, 4H), 1.72 (s, 4H), 1.59 (dq, *J* = 9.9, 5.1 Hz, 2H), 1.36 (s, 5H), 0.91 (dd, *J* = 12.3, 6.1 Hz, 12H).

HRESIMS [M+H] Calcd. for C<sub>26</sub>H<sub>50</sub>N<sub>10</sub>O<sub>6</sub>Cl<sub>2</sub><sup>+</sup>, 627.2689; Measured: 627.2692

#### **tert-butyl (3-chloro-5-((4-(phenylsulfonamido)phenyl)amino)phenyl)-L-leucinate (19)**

To a stirred solution of **15** (30 mg, 0.09 mmol) in THF and water (5 mL, 0.5 mL) was added **18a** (22 mg, 0.09 mmol, 1 equiv), and potassium carbonate (19 mg, 0.18 mmol, 1.35 equiv). This was left to stir at room temperature overnight. EtOAc and water (50 mL) were added to the mixture, and the organic layers separated. The aqueous layer was washed with EtOAc (50 mL ×3), and the organic layers combined and washed with water (30 mL ×2) and brine (20 mL), dried over anhydrous MgSO<sub>4</sub>, and concentrated in vacuo. The crude product was purified by column chromatography MeOH/DCM (0–8%) to yield a beige solid (28mg, 57% yield)

<sup>1</sup>H NMR (600 MHz, Chloroform-*d*) δ 7.74 – 7.73 (m, 1H), 7.73 (d, *J* = 1.5 Hz, 1H), 7.46 (d, *J* = 1.7 Hz, 2H), 7.45 (d, *J* = 2.1 Hz, 3H), 7.44 (d, *J* = 1.8 Hz, 1H), 7.03 (dd, *J* = 10.8, 8.8 Hz, 3H), 2.08 (d, *J* = 35.1 Hz, 1H), 1.71 (ddd, *J* = 19.4, 13.5, 6.2 Hz, 2H), 1.43 (d, *J* = 7.8 Hz, 9H), 1.28 – 1.24 (m, 1H), 0.97 (dd, *J* = 6.5, 4.7 Hz, 6H).

HRESIMS [M+H] Calcd. for C<sub>25</sub>H<sub>32</sub>N<sub>6</sub>O<sub>4</sub>SCl<sup>+</sup> 547.1889; measured: 547.1898

#### **tert-butyl (4-((4-(butylsulfonamido)phenyl)amino)-6-chloro-1,3,5-triazin-2-yl)-L-leucinate (20)**

To a stirred solution of **15** (50 mg, 0.15 mmol) in THF and water (5 mL, 0.5 mL) was added **18b** (34 mg, 0.15 mmol, 1 equiv), and potassium carbonate (31 mg, 0.22 mmol, 1.35 equiv). This was left to stir at room temperature overnight. EtOAc and water (50 mL) were added to the mixture, and the organic layers separated. The aqueous layer was washed with EtOAc (50 mL ×3), and the organic layers combined and washed with water (30 mL ×2) and brine (20 mL), dried over anhydrous MgSO<sub>4</sub>, and concentrated in vacuo. The crude product was purified by column chromatography MeOH/DCM (0–5%) to yield a pale yellow solid (30mg, 39% yield)

<sup>1</sup>H NMR (600 MHz, Chloroform-*d*) δ 7.56 – 7.51 (m, 2H), 7.23 – 7.18 (m, 2H), 4.13 (q, *J* = 7.1 Hz, 1H), 3.10 – 3.06 (m, 2H), 2.18 (s, 2H), 1.49 (s, 4H), 1.46 – 1.40 (m, 9H), 1.25 (d, *J* = 4.1 Hz, 1H), 0.99 (d, *J* = 1.6 Hz, 2H), 0.98 (d, *J* = 1.5 Hz, 2H), 0.94 – 0.91 (m, 6H). <sup>13</sup>C NMR (151 MHz, CDCl<sub>3</sub>) δ 132.57, 131.00, 128.92, 122.49, 122.27, 121.90, 82.40, 77.34, 77.13, 76.91, 68.28, 60.52, 53.11, 51.43, 41.91, 41.44, 31.05, 30.47, 29.04, 28.14, 28.10, 25.64, 25.05, 25.00, 23.86, 23.10, 23.00, 22.81, 22.31, 22.17, 21.56, 21.17, 14.32, 14.17, 13.68, 13.66, 11.08.

<sup>13</sup>C NMR (151 MHz, CDCl<sub>3</sub>) δ 132.57, 131.00, 128.92, 122.49, 122.27, 121.90, 82.40, 77.34, 77.13, 76.91, 68.28, 60.52, 53.11, 51.43, 41.91, 41.44, 31.05, 30.47, 29.04, 28.14, 28.10, 25.64, 25.05, 25.00, 23.86, 23.10, 23.00, 22.81, 22.31, 22.17, 21.56, 21.17, 14.32, 14.17, 13.68, 13.66, 11.08.

HRESIMS [M+H] Calcd. for C<sub>23</sub>H<sub>36</sub>N<sub>6</sub>O<sub>4</sub>SCl<sup>+</sup> 527.2202; measured: 527.2197

### **tert-butyl 4-((4-acetamidophenyl)amino)-6-chloro-1,3,5-triazin-2-yl)-L-leucinate (21)**

To a stirred solution of **15** (56 mg, 0.167 mmol) in THF and water (5 mL, 0.5 mL) was added **18c** (25 mg, 0.167 mmol, 1 equiv), and potassium carbonate (35 mg, 0.2505 mmol, 1.35 equiv). This was left to stir at room temperature for 5h. EtOAc and water (50 mL) were added to the mixture, and the organic layers separated. The aqueous layer was washed with EtOAc (50 mL ×3), and the organic layers combined and washed with water (30 mL ×2) and brine (20 mL), dried over anhydrous MgSO<sub>4</sub>, and concentrated in vacuo. The crude product was purified by column chromatography MeOH/DCM (0–8%) to yield a white solid (35mg, 47% yield).

<sup>1</sup>H NMR (600 MHz, Chloroform-*d*) δ 7.50 (s, 2H), 7.48 (s, 1H), 7.12 (s, 2H), 2.19 (d, *J* = 1.9 Hz, 3H), 2.05 (s, 1H), 1.76 – 1.68 (m, 2H), 1.46 (d, *J* = 29.1 Hz, 9H), 1.26 (t, *J* = 7.1 Hz, 1H), 1.00 – 0.92 (m, 6H). HRESIMS [M+H] Calcd. for C<sub>21</sub>H<sub>30</sub>ClN<sub>6</sub>O<sub>3</sub><sup>+</sup> 449.1990; measured: 449.2062

### **tert-butyl 4-((4-benzamidophenyl)amino)-6-chloro-1,3,5-triazin-2-yl)-L-leucinate (22)**

To a stirred solution of **15** (56 mg, 0.167 mmol) in THF and water (5 mL, 0.5 mL) was added **18d** (35 mg, 0.167 mmol, 1 equiv), and potassium carbonate (35 mg, 0.2505 mmol, 1.35 equiv). This was left to stir at room temperature for 5h. EtOAc and water (50 mL) were added to the mixture, and the organic layers separated. The aqueous layer was washed with EtOAc (50 mL ×3), and the organic layers combined and washed with water (30 mL ×2) and brine (20 mL), dried over anhydrous MgSO<sub>4</sub>, and concentrated in vacuo. The crude product was purified by column chromatography MeOH/DCM (0–8%) to yield a yellow solid (52 mg, 61% yield)

<sup>1</sup>H NMR (600 MHz, Chloroform-*d*) δ 7.88 (dd, *J* = 8.4, 1.4 Hz, 2H), 7.81 (d, *J* = 5.2 Hz, 1H), 7.64 (dd, *J* = 13.2, 8.7 Hz, 2H), 7.57 (dd, *J* = 10.6, 3.5 Hz, 2H), 7.51 (td, *J* = 7.5, 1.8 Hz, 2H), 4.67 – 4.46 (m, 1H), 1.77 – 1.66 (m, 1H), 1.47 (d, *J* = 28.4 Hz, 9H), 1.32 – 1.20 (m, 1H), 1.00 – 0.92 (m, 6H), 0.90 – 0.80 (m, 1H).

HRESIMS [M+H] Calcd. for C<sub>26</sub>H<sub>32</sub>N<sub>6</sub>O<sub>3</sub>Cl<sup>+</sup> 511.2219; measured: 511.2206

### **tert-butyl 4-chloro-1,3,5-triazin-2-yl)-L-leucinate (24)**

L-Leucine tert-butyl ester hydrochloride was washed with sodium carbonate 3 times to yield L-leucine tert butyl ester. A solution of 2,4-dichloro-1,3,5-triazine (250 mg, 1.67 mmol) in tetrahydrofuran (5 mL) was cooled to 10°C by an ice-salt bath, and then L-leucine tert-butyl ester (372 mg, 1.67 mmol) in tetrahydrofuran (5 mL) was added slowly and the mixture was stirred at room temperature for 30 min. EtOAc and water (50 mL) were added to the mixture, and the organic layers separated. The aqueous layer was washed with EtOAc (50 mL ×3), and the organic layers combined and washed with water (30 mL ×2) and brine (20 mL), dried over anhydrous MgSO<sub>4</sub>, and concentrated in vacuo. The crude product was purified by column chromatography MeOH/DCM (0–10%) to give a white solid (279 mg, 49% yield)

### **tert-butyl 4-((4-(butylsulfonamido)phenyl)amino)-1,3,5-triazin-2-yl)-L-leucinate (25)**

To a stirred solution of **24** (50 mg, 0.167 mmol) in THF and water (5 mL, 0.5 mL) was added **18b** (40 mg, 0.15 mmol, 1 equiv), and potassium carbonate (31 mg, 0.22 mmol, 1.35 equiv). This was left to stir at room temperature overnight. EtOAc and water (50 mL) were added to the mixture, and the organic layers separated. The aqueous layer was washed with EtOAc (50 mL ×3), and the organic layers combined and washed with water (30 mL ×2) and brine (20 mL), dried over anhydrous MgSO<sub>4</sub>,

and concentrated in vacuo. The crude product was purified by column chromatography MeOH/DCM (0–8%) to yield a yellow solid (29 mg, 34% yield)

$^1\text{H}$  NMR (600 MHz, Chloroform-*d*)  $\delta$  8.25 (d,  $J$  = 29.2 Hz, 1H), 7.71 (dd,  $J$  = 5.7, 3.3 Hz, 1H), 7.60 – 7.53 (m, 2H), 7.20 (dd,  $J$  = 8.7, 6.6 Hz, 1H), 6.21 (d,  $J$  = 3.9 Hz, 1H), 4.72 – 4.47 (m, 1H), 4.22 (qd,  $J$  = 10.9, 5.9 Hz, 2H), 3.09 – 3.05 (m, 2H), 2.98 (d,  $J$  = 43.5 Hz, 0H), 1.84 – 1.67 (m, 2H), 1.49 – 1.40 (m, 9H), 1.30 (d,  $J$  = 12.4 Hz, 2H), 1.01 – 0.94 (m, 3H), 0.95 – 0.88 (m, 6H).

HRESIMS [M+H] Calcd. for  $\text{C}_{23}\text{H}_{37}\text{N}_6\text{O}_4\text{S}^+$  493.2592; measured 493.2590

#### **tert-butyl 4-((4-acetamidophenyl)amino)-1,3,5-triazin-2-yl)-L-leucinate (26)**

To a stirred solution of **24** (50 mg, 0.167 mmol) in THF and water (5 mL, 0.5 mL) was added **18c** (25 mg, 0.15 mmol, 1 equiv), and potassium carbonate (31 mg, 0.22 mmol, 1.35 equiv). This was left to stir at room temperature overnight. EtOAc and water (50 mL) were added to the mixture, and the organic layers separated. The aqueous layer was washed with EtOAc (50 mL  $\times$ 3), and the organic layers combined and washed with water (30 mL  $\times$ 2) and brine (20 mL), dried over anhydrous  $\text{MgSO}_4$ , and concentrated in vacuo. The crude product was purified by column chromatography MeOH/DCM (0–10%) to give a beige solid (33 mg, 48% yield).

$^1\text{H}$  NMR (600 MHz, Chloroform-*d*)  $\delta$  8.23 (d,  $J$  = 31.1 Hz, 1H), 7.58 – 7.44 (m, 3H), 7.20 (s, 1H), 5.78 (s, 1H), 4.64 (q,  $J$  = 3.4 Hz, 0H), 4.54 (td,  $J$  = 8.5, 5.8 Hz, 1H), 2.18 (d,  $J$  = 2.8 Hz, 3H), 1.52 – 1.49 (m, 2H), 1.44 (s, 6H), 1.26 (s, 1H), 1.02 – 0.93 (m, 9H).  $^{13}\text{C}$  NMR (151 MHz, Chloroform-*d*)  $\delta$  172.23, 169.61, 168.21, 165.08, 121.42, 120.59, 82.01, 53.04 (d,  $J$  = 17.9 Hz), 41.73 (d,  $J$  = 48.5 Hz), 28.12, 25.04 (d,  $J$  = 13.1 Hz), 24.65, 22.97, 22.86, 22.35.

$^{13}\text{C}$  NMR (151 MHz, Chloroform-*d*)  $\delta$  172.23, 169.61, 168.21, 165.08, 121.42, 120.59, 82.01, 53.04 (d,  $J$  = 17.9 Hz), 41.73 (d,  $J$  = 48.5 Hz), 28.12, 25.04 (d,  $J$  = 13.1 Hz), 24.65, 22.97, 22.86, 22.35.

HRESIMS [M+H] Calcd. for  $\text{C}_{21}\text{H}_{31}\text{N}_6\text{O}_3^+$  452.2452; measured 452.2456.

#### **4-((4-acetamidophenyl)amino)-1,3,5-triazin-2-yl)-L-leucine (27)**

To a suspension of **26** (130 mg, 0.314 mmol) in  $\text{CH}_2\text{Cl}_2$  (1 mL) at r.t. was added trifluoroacetic acid (0.2 mL) and the mixture stirred at r.t. for 3h (TLC, LCMS). The solvent was then removed *in vacuo* (in fume hood), and the residue triturated with *c*-Hex:Et<sub>2</sub>O, 1:1. The solid formed was collected by filtration, azeotroped (DCE, 10 mL  $\times$ 2) and dried to afford the title compound as a white solid (0.08 g, 0.223 mmol, 71%).

$^1\text{H}$ NMR (600 MHz, DMSO-*d*<sub>6</sub>)  $\delta$ /ppm: 9.85 (m, 1H), 8.20 (m, 1H), 7.58 (d, 1H,  $J$  = 8.3 Hz), 7.51-7.47 (m, 2H), 4.44 (m, 1H), 2.02 (s, 3H), 1.76-1.68 (m, 2H), 0.92 (d, 3H,  $J$  = 6.3 Hz), 0.88-0.85 (m, 3H).

$^{13}\text{C}$ NMR (150 MHz, DMSO-*d*<sub>6</sub>)  $\delta$ /ppm: 174.5, 174.1, 168.0, 134.7, 133.9, 120.6, 119.8, 119.2, 51.9, 24.5, 23.9, 23.0, 22.9, 21.3, 21.1.

LCMS [M+H] Calcd. for:  $\text{C}_{17}\text{H}_{23}\text{N}_6\text{O}_3^+$  359.18; measured: 359.20

#### **Isopropyl 4-((4-acetamidophenyl)amino)-1,3,5-triazin-2-yl)-L-leucinate (28)**

A solution of **27** (100 mg, 0.279 mmol),  $\text{CBr}_4$  (92.5 mg, 0.279 mmol) and anhydrous *i*PrOH (5 mL) was heated in the microwave at 150°C for 3h. After the reaction was complete (analysis by TLC), the excess alcohol was removed *in vacuo*. Further purification was achieved by flash chromatography with ethyl acetate/hexane. Column chromatography (19:1,  $\text{CH}_2\text{Cl}_2$ :MeOH) afforded the title compound as a white solid (0.043 g, 0.107 mmol, 38%).

$^1\text{H}$  NMR (600 MHz, DMSO- $d_6$ )  $\delta$ /ppm: 9.85 (m, 1H), 8.15 (d, 1H,  $J$  = 12.9 Hz), 7.59 (d, 1H,  $J$  = 8.8 Hz), 7.51-7.46 (m, 2H), 4.88 (m, 1H), 4.40 (m, 1H), 3.35 (s, 6H), 2.01 (s, 3H), 1.75-1.68 (m, 2H), 1.52 (m, 1H), 1.18 (d, 1H,  $J$  = 6.2 Hz), 1.15 (dd, 3H,  $J$  = 6.1, 3.8 Hz), 0.92 (d, 3H,  $J$  = 6.3 Hz), 0.86 (t, 3H,  $J$  = 6.4 Hz).

$^{13}\text{C}$  NMR (150 MHz, DMSO- $d_6$ )  $\delta$ /ppm: 172.7, 167.9, 165.6, 164.9, 134.6, 134.2, 119.2, 119.0, 68.0, 67.8, 52.1, 24.5, 24.4, 24.0, 22.9, 22.8, 21.6, 21.5, 21.3, 21.2.

LCMS [M+H] Calcd. For  $\text{C}_{20}\text{H}_{29}\text{N}_6\text{O}_3$ : 401.2; measured: 401.2

#### **cyclopentyl(4-((4-acetamidophenyl)amino)-1,3,5-triazin-2-yl)-L-leucinate (29)**

A solution of the **27** (100 mg, 0.279 mmol),  $\text{CBr}_4$  (92.5 mg, 0.279 mmol) and anhydrous *c*-Pentanol (2 mL) was irradiated in the MW at 150°C for 1h. After the reaction was complete (analysis by TLC), the excess alcohol was removed *in vacuo*. Column chromatography (19:1,  $\text{CH}_2\text{Cl}_2$ :MeOH) afforded the title compound as a white solid (0.014 g, 0.033 mmol, 24%).

$^1\text{H}$  NMR (600 MHz, DMSO- $d_6$ )  $\delta$ /ppm: 9.85 (d, 1H,  $J$  = 10.0 Hz), 8.15 (d, 1H,  $J$  = 13.9 Hz), 7.57 (d, 1H,  $J$  = 8.9 Hz), 7.50-7.45 (m, 2H), 5.06 (m, 1H), 5.03 (m, 1H), 4.42-4.34 (m, 2H), 2.01 (s, 3H), 1.75-1.68 (m, 3H), 1.57-1.43 (m, 5H), 0.92 (d, 3H,  $J$  = 6.3 Hz), 0.86 (dd, 3H,  $J$  = 6.3, 3.7 Hz).

$^{13}\text{C}$  NMR (150 MHz, DMSO- $d_6$ )  $\delta$ /ppm: 172.7, 165.1, 134.2, 120.6, 77.1, 52.5, 41.8, 41.5, 32.8, 32.6, 29.8, 25.04, 24.95, 24.7, 23.8, 23.7, 22.96, 22.87, 22.3, 22.1.

LCMS [M-H] Calcd. for  $\text{C}_{22}\text{H}_{29}\text{N}_6\text{O}_3^-$  425.24; measured 425.80

#### **(S)-2-((4-((4-acetamidophenyl)amino)-1,3,5-triazin-2-yl)amino)-N-methoxy-N,4-dimethylpentanamide (32)**

To a solution of **30** (167 mg, 0.632 mmol) and Weinreb amide L-leucine HCl (200 mg, 0.949 mmol) in dry DMF (2 mL) at r.t. was added triethylamine (0.22 mL, 1.58 mmol) and the mixture stirred at 80°C for 3h (TLC, LCMS). To the reaction was then added water, and the resultant solid was filtered, washed with water and then dried. Column chromatography (19:1,  $\text{CH}_2\text{Cl}_2$ :MeOH) afforded the title compound as a white solid (0.038 g, 0.094 mmol, 15%).

$^1\text{H}$  NMR (600 MHz,  $\text{CDCl}_3$ )  $\delta$ /ppm: 8.22 (m, 1H), 7.51 (d, 2H,  $J$  = 8.8 Hz), 7.47-7.41 (m, 2H), 5.28 (m, 1H), 3.91 (s, 1H), 3.61 (s, 1H), 3.22 (m, 3H), 2.18 (d, 3H,  $J$  = 5.9 Hz), 1.76 (m, 1H), 1.66-1.56 (m, 4H), 1.00-0.90 (m, 5H)

LCMS [M+H] Calcd. for  $\text{C}_{19}\text{H}_{28}\text{N}_7\text{O}_3^+$  402.22; measured: 402.10

#### **(S)-N-(4-((4-((1-hydroxy-4-methylpentan-2-yl)amino)-1,3,5-triazin-2-yl)amino)phenyl)acetamide (33)**

To a solution of **30** (100 mg, 0.379 mmol) and L-leucinol (63.5 mg, 0.541 mmol) in dry DMF (2 mL) at r.t. was added triethylamine (0.056 mL, 0.397 mmol) and the mixture stirred at 80°C for 3h (TLC, LCMS). To the reaction was then added water, and the resultant solid was filtered, washed with water and then dried. Column chromatography (4:1, EtOAc:*c*-Hex  $\rightarrow$  EtOAc  $\rightarrow$  9:1, EtOAc:MeOH) afforded the title compound as a white solid (0.029 g, 0.084 mmol, 23%).

$^1\text{H}$  NMR (600 MHz, DMSO)  $\delta$ /ppm: 9.83 (s, 1H), 9.43 (m, 1H), 7.68 (s, 1H), 7.63 (d, 1H,  $J$  = 7.7 Hz), 7.45 (dd, 2H,  $J$  = 8.9, 4.0 Hz), 4.71-4.67 (m, 2H), 2.01 (s, 3H), 1.63 (m, 1H), 1.38 (m, 2H), 0.89 (dd, 3H,  $J$  = 6.5, 3.4 Hz), 0.87=0.84 (m, 3H).

$^{13}\text{C}$  NMR (150 MHz, DMSO)  $\delta$ /ppm: 167.9, 165.4, 164.9, 134.9, 134.0, 119.1, 63.9, 63.5, 59.8, 55.0, 50.1, 29.0, 24.4, 23.9, 23.5, 22.2, 21.9.

LCMS [M+H] Calcd. for  $\text{C}_{17}\text{H}_{25}\text{N}_6\text{O}_2^+$  345.20; measured 345.30.

***tert*-butyl 4-((4-acetamidophenyl)amino)-1,3,5-triazin-2-yl)-D-leucinate (34)**

To a solution of **30** (100 mg, 0.379 mmol) and t-Bu D-leucine HCl (121 mg, 0.54 mmol) in dry DMF (2 mL) at r.t. was added triethylamine (0.126 mL, 0.9 mmol) and the mixture stirred at 80°C for 3h (TLC, LCMS). To the reaction was then added water, and the resultant solid was filtered, washed with water and then dried. Column chromatography (7:3, EtOAc:cHex) followed by reverse phase column chromatography (11:9, MeCN:H<sub>2</sub>O) afforded the title compound as a white solid (0.079 g, 0.191 mmol, 50%).

$^1\text{H}$  NMR (600 MHz, DMSO-*d*<sub>6</sub>)  $\delta$ /ppm: 9.82 (s, 1H), 9.52 (m, 1H), 8.14 (m, 1H), 7.87 (s, 1H), 7.69 (s, 1H), 7.61 (d, 1H, *J* = 8.6 Hz), 7.52-7.46 (m, 2H), 4.33 (m, 1H), 2.01 (s, 3H), 1.76-1.65 (m, 2H), 1.52 (m, 1H), 1.39 (s, 3H), 1.35 (s, 6H), 0.92 (m, 3H), 0.86 (m, 3H).

$^{13}\text{C}$  NMR (150 MHz, DMSO-*d*<sub>6</sub>)  $\delta$ /ppm: 172.4, 172.3, 167.9, 165.6, 165.0, 134.6, 134.2, 119.3, 119.0, 80.4, 52.6, 27.7, 27.6, 24.6, 24.4, 23.9, 22.9, 22.8, 21.34, 21.28.

LCMS [M+H] Calcd. for  $\text{C}_{21}\text{H}_{31}\text{N}_6\text{O}_3^+$  415.24; measured: 415.30.

***tert*-butyl 4-((4-acetamidophenyl)amino)-1,3,5-triazin-2-yl)-L-valinate (35)**

To a solution of **30** (100 mg, 0.379 mmol) and t-Bu valine HCl (113 mg, 0.54 mmol) in dry DMF (2 mL) was added triethylamine (0.126 mL, 0.9 mmol) at r.t. and the mixture stirred at 80°C for 3h (TLC, LCMS). The reaction was cooled, water was added, and the resultant solid was filtered, washed with water and then diethyl ether and dried. Reverse phase column chromatography (2:3, MeCN:H<sub>2</sub>O) afford the title compound as a white solid (0.040 g, 0.100 mmol, 26%).

$^1\text{H}$  NMR (600 MHz, CDCl<sub>3</sub>)  $\delta$ /ppm: 8.22 (m, 1H), 7.56-7.40 (m, 4H), 6.01 (s, 1H), 4.46 (m, 1H), 2.25 (m, 1H), 2.18 (s, 3H), 1.48 (s, 3H), 1.46 (s, 6H), 1.04-0.97 (m, 6H).

$^{13}\text{C}$  NMR (150 MHz, CDCl<sub>3</sub>)  $\delta$ /ppm: 171.0, 168.3, 166.1, 165.6, 165.3, 134.3, 133.7, 120.6, 82.2, 59.4, 59.1, 31.6, 31.3, 28.2, 24.6, 18.3, 18.1

LCMS [M+H] Calcd. for  $\text{C}_{20}\text{H}_{29}\text{N}_6\text{O}_3^+$  401.22; measured 401.30.

***tert*-butyl 4-((4-acetamidophenyl)amino)-1,3,5-triazin-2-yl)glycinate (36)**

To a solution of **30** (100 mg, 0.379 mmol) and t-Bu glycine HCl (95 mg, 0.569 mmol) in dry DMF (2 mL) at r.t. was added triethylamine (0.133 mL, 0.95 mmol) and the mixture stirred at 80°C for 3h (TLC, LCMS). To the reaction was then added water, and the resultant solid was filtered, washed with water and then dried. Column chromatography (1:4, c-Hex, EtOAc) afforded the title compound as a white solid (0.036 g, 0.173 mmol, 46%).

$^1\text{H}$  NMR (600 MHz, DMSO-*d*<sub>6</sub>)  $\delta$ /ppm: 9.82 (s, 1H), 9.54 (d, br, *J* = 48.0 Hz, 1H), 8.16 (d, *J* = 30.0 Hz, 1H), 7.54-7.94 (m, 3H), 7.44-7.52 (m, 2H), 3.85-3.93 (m, 2H), 2.02 (s, 3H), 1.41 (s, 3H), 1.37 (s, 6H).

$^{13}\text{C}$  NMR (150 MHz, DMSO-*d*<sub>6</sub>)  $\delta$ /ppm: 169.3 (d, *J* = 19.5 Hz), 167.8, 165.6 (d, *J* = 19.5 Hz), 165.2, 165.1, 134.6, 134.2, 120.2 (d, *J* = 54.0 Hz), 119.0 (d, *J* = 54.0 Hz), 80.6 (d, *J* = 7.5 Hz), 42.7, 27.7 (d, *J* = 10.5 Hz), 23.8 (d, *J* = 4.5 Hz).

LCMS [M+H] Calcd. for:  $\text{C}_{17}\text{H}_{23}\text{N}_6\text{O}_3^+$  359.18; measured: 359.20.

***tert*-butyl (S)-2-((4-((4-acetamidophenyl)amino)-1,3,5-triazin-2-yl)amino)-3,3-dimethylbutanoate (37)**

To a solution of **30** (100 mg, 0.379 mmol) and H-Tle-OtBu HCl (127 mg, 0.569 mmol) in dry DMF (2 mL) at r.t. was added triethylamine (0.133 mL, 0.948 mmol) and the mixture stirred at 80°C for 3h (TLC, LCMS). To the reaction was then added water, and the resultant solid was filtered, washed with water and then dried. Column chromatography (9:1, CH<sub>2</sub>Cl<sub>2</sub>:MeOH) followed by reverse phase column chromatography (1:1, MeCN:H<sub>2</sub>O) afforded the title compound as a white solid (0.011 g, 0.027 mmol, 7%).

<sup>1</sup>H NMR (600 MHz, DMSO-d<sub>6</sub>) δ/ppm: 9.86 (s, 1H), 9.57 (m, 1H), 8.16 (m, 1H), 7.63 (d, 2H, J = 7.0 Hz), 7.50 (d, 2H, J = 8.8 Hz), 4.16 (s, 1H), 2.01 (m, 3H), 1.41 (s, 3H), 1.35 (s, 6H), 1.04 (s, 6H), 1.03 (s, 3H).

LCMS [M+H] Calcd. for C<sub>21</sub>H<sub>31</sub>N<sub>6</sub>O<sub>3</sub><sup>+</sup> 415.24; measured: 414.90

***tert*-butyl 2-((4-((4-acetamidophenyl)amino)-1,3,5-triazin-2-yl)amino)-2-methylpropanoate (38)**

To a solution of **30** (75 mg, 0.284 mmol) and HAib-OtBu (48 mg, 0.301 mmol) in dry DMF (2 mL) at r.t. was added potassium carbonate (43 mg, 0.312 mmol) and the mixture stirred at 80°C for 3 h. The reaction was then cooled and partitioned between EtOAc and water, and the organic layer washed with sat. aq. LiCl. The organic layer was then dried and evaporated. Column chromatography (19:1, CH<sub>2</sub>Cl<sub>2</sub>:MeOH) followed by reverse phase column chromatography (3:7, MeCN:H<sub>2</sub>O) afforded the title compound as a white solid (0.011 g, 0.029 mmol, 10%).

<sup>1</sup>H NMR (600 MHz, DMSO-d<sub>6</sub>) δ/ppm: 9.81 (m, 1H), 8.12 (m, 1H), 7.56 (d, 2H, J = 8.9 Hz), 7.47 (t, 2H, J = 8.3 Hz), 2.01 (s, 3H), 1.48 (s, 4H), 1.43 (s, 2H), 1.33 (s, 3H), 1.22 (s, 6H).

LCMS [M+H] Calcd. For C<sub>19</sub>H<sub>27</sub>N<sub>6</sub>O<sub>3</sub><sup>+</sup> 387.21; measured: 387.20

***tert*-butyl (4-((4-acetamidophenyl)amino)-1,3,5-triazin-2-yl)-L-alaninate (39)**

To a solution of **30** (100 mg, 0.379 mmol) and t-Bu alanine HCl (103 mg, 0.568 mmol) in dry DMF (2 mL) at r.t. was added dry triethylamine (0.133 mL, 0.948 mmol) and the mixture stirred at 80°C for 3h (TLC, LCMS). The reaction was cooled, water was added, and the resultant solid was filtered, washed with water and then dried. Column chromatography (8:2, EtOAc:cHex) followed by reverse phase column chromatography (1:1, MeCN:H<sub>2</sub>O) afforded the *title compound* as a white solid (0.035 g, 0.094 mmol, 25%).

<sup>1</sup>H NMR (600 MHz, DMSO-d<sub>6</sub>) δ/ppm: 9.82 (s, 1H), 9.52 (m, 1H), 9.15 (m, 1H), 7.59 (d, 2H, J = 9.0 Hz), 7.52-7.47 (m, 2H), 4.31 (m, 1H), 2.02 (s, 3H), 1.39 (s, 3H), 1.38-1.30 (m, 9H).

<sup>13</sup>C NMR (150 MHz, DMSO-d<sub>6</sub>) δ/ppm: 172.4, 167.9, 165.5, 164.7, 134.6, 134.2, 119.3, 119.0, 80.4, 49.8, 27.7, 24.0, 17.0.

LCMS [M+H] Calcd. for C<sub>18</sub>H<sub>25</sub>N<sub>6</sub>O<sub>3</sub><sup>+</sup> 373.19; measured 373.20.

***tert*-butyl (S)-2-((4-((4-acetamidophenyl)amino)-1,3,5-triazin-2-yl)amino)-2-cyclohexylacetate (40)**

To a solution of **30** (100 mg, 0.379 mmol) and H-L-Cyclohexyl-Gly-OtBu·HCl (142 mg, 0.569 mmol) in dry DMF (2 mL) at r.t. was added triethylamine (0.133 mL, 0.948 mmol) and the mixture stirred at 80°C for 3h (TLC, LCMS). To the reaction was then added water, and the resultant solid was filtered, washed with water and then dried. Column chromatography (9:1, CH<sub>2</sub>Cl<sub>2</sub>:MeOH) followed by reverse phase column chromatography (11:9, MeCN:H<sub>2</sub>O) afforded the title compound as a white solid (0.046 g, 0.104 mmol, 28%).

$^1\text{H}$  NMR (600 MHz, DMSO- $d_6$ )  $\delta$ /ppm: 9.86 (s, 1H), 9.56 (s, 1H), 8.14 (m, 1H), 7.76 (m, 1H), 7.61 (d, 2H,  $J = 8.1$  Hz), 7.53-7.48 (m, 2H), 4.24 (t, 1H,  $J = 7.4$  Hz), 2.02 (s, 3H), 1.85-1.56 (m, 6H), 1.40 (s, 3H), 1.34 (s, 6H), 1.26-1.07 (m, 5H).

$^{13}\text{C}$  NMR (150 MHz, DMSO- $d_6$ )  $\delta$ /ppm: 171.2, 167.9, 165.5, 165.1, 165.0, 134.6, 134.2, 120.0, 119.0, 80.5, 59.2, 29.0, 28.8, 28.7, 27.7, 25.6, 24.0.

LCMS [M+H] Calcd. for  $\text{C}_{23}\text{H}_{33}\text{N}_6\text{O}_3^+$  441.25; measured 440.90.

#### ***tert*-butyl (4-((4-acetamidophenyl)amino)-1,3,5-triazin-2-yl)-L-phenylalaninate (41)**

To a solution of **30** (100 mg, 0.379 mmol) and *t*-OBu phenyl alanine HCl (140 mg, 0.542 mmol) in dry DMF (2 mL) at r.t. was added triethylamine (0.127 mL, 0.902 mmol) and the mixture stirred at 80°C for 3h (TLC, LCMS). To the reaction was then added water, and the resultant solid was filtered, washed with water and then dried. Reverse phase column chromatography (9:11, MeCN:H<sub>2</sub>O) afford the title compound as a white solid (0.073 g, 0.163 mmol, 43%).

$^1\text{H}$  NMR (600 MHz, DMSO- $d_6$ )  $\delta$ /ppm: 9.87 (s, 1H), 9.56 (m, 1H), 8.16 (m, 1H), 7.61 (d, 2H,  $J = 8.7$  Hz), 7.54 (d, 1H,  $J = 8.8$  Hz), 7.52 (d, 1H,  $J = 8.8$  Hz), 7.34-7.31 (m, 4H), 7.25 (m, 1H), 4.54 (s, 1H), 3.12-3.08 (m, 2H), 2.06 (s, 3H), 1.37 (s, 3H), 1.34 (s, 6H).

$^{13}\text{C}$  NMR (150 MHz, DMSO- $d_6$ )  $\delta$ /ppm: 171.3, 167.9, 165.6, 164.9, 164.8, 158.4, 137.8, 134.5, 134.3, 129.1, 128.3, 126.5, 119.3, 119.0, 80.7, 80.6, 55.8, 27.6, 27.5, 23.9.

LCMS [M+H] Calcd. for  $\text{C}_{24}\text{H}_{29}\text{N}_6\text{O}_3^+$  449.22; measured 449.30

#### ***tert*-butyl (4-((4-acetamidophenyl)amino)-1,3,5-triazin-2-yl)-L-tyrosinate (42)**

To a solution of **30** (75 mg, 0.284 mmol) and *t*-OBu tyrosine (71 mg, 0.298 mmol) in dry DMF (2 mL) at room temperature was added potassium carbonate (43 mg, 0.312 mmol) and the mixture stirred at 80°C for 3h. The reaction was cooled and partitioned between ethyl acetate and saturated citric acid. The organic layer was washed with saturated aqueous lithium chloride, dried and evaporated. Column chromatography (30:1, CH<sub>2</sub>Cl<sub>2</sub>:MeOH) followed by reverse phase column chromatography (2:3, MeCN:H<sub>2</sub>O) afforded the title compound as a white solid (0.020 g, 0.043 mmol, 15%).

$^1\text{H}$  NMR (600 MHz, DMSO- $d_6$ )  $\delta$ /ppm: 9.86 (m, 1H), 9.23 (m, 1H), 8.12 (m, 1H), 7.58 (d, 2H,  $J = 8.5$  Hz), 7.53-7.46 (m, 2H), 7.10-7.02 (m, 2H), 6.66 (m, 2H), 4.39 (m, 1H), 3.00-2.87 (m, 2H), 2.02 (s, 3H), 1.33 (s, 3H), 1.30 (s, 6H).

$^{13}\text{C}$  NMR (150 MHz, DMSO- $d_6$ )  $\delta$ /ppm: 174.5, 172.8, 170.0, 153.9, 134.3, 133.4, 141.7, 130.3, 129.6, 119.1, 114.8, 114.1, 80.0, 67.5, 59.8, 56.2, 42.7, 33.1, 27.9, 27.7, 27.5, 23.9, 21.2, 14.2.

LCMS [M+H] Calcd. for  $\text{C}_{24}\text{H}_{29}\text{N}_6\text{O}_4^+$  464.22; measured: 465.20.

#### ***tert*-butyl (S)-2-((4-((4-acetamidophenyl)amino)-1,3,5-triazin-2-yl)amino)-3-(4-fluorophenyl)propanoate (43)**

To a solution of **30** (50 mg, 0.190 mmol) and 4-Fluorophenylalanine-OtBu HCl (58 mg, 0.209 mmol) in dry DMF (1 mL) at r.t. was added triethylamine (0.059 mL, 0.417 mmol) and the mixture stirred at 80°C for 3h (TLC, LCMS). To the reaction was then added water, and the resultant solid was filtered, washed with water and then dried. Reverse phase column chromatography (3:2, MeCN:H<sub>2</sub>O) afforded the title compound as a white solid (0.014 g, 0.030 mmol, 16%).

$^1\text{H}$  NMR (600 MHz, DMSO- $d_6$ )  $\delta$ /ppm: 9.84 (s, 1H), 8.11 (m, 1H), 7.57 (d, 1H,  $J = 8.8$  Hz), 7.52-7.46 (m, 2H), 7.36-7.30 (m, 2H), 7.11 (t, 2H,  $J = 8.7$  Hz), 4.46 (m, 1H), 3.09-3.00 (m, 2H), 2.02 (s, 3H), 1.33 (s, 3H), 1.30 (s, 6H)

$^{13}\text{C}$  NMR (150 MHz, DMSO- $d_6$ )  $\delta$ /ppm: 171.1, 167.9, 165.6, 164.92, 164.85, 160.3, 134.5, 134.3, 134.0, 131.03, 130.98, 119.3, 119.0, 115.0, 114.9, 80.8, 80.7, 27.6, 27.5, 23.9.

LCMS theoretical [ $\text{C}_{24}\text{H}_{27}\text{FN}_6\text{O}_3 + \text{H}$ ] 467.21; measured: 468.30.

**tert-butyl (S)-3-((4-((4-acetamidophenyl)amino)-1,3,5-triazin-2-yl)amino)-4-phenylbutanoate (44)**

To a solution of **30** (100 mg, 0.379 mmol) and *tert*-Butyl (3S)-3-amino-4-phenylbutanoate (98 mg, 0.413 mmol) in dry DMF (2 mL) at r.t. was added triethylamine (0.06 mL) and the mixture stirred at 80°C for 3h (TLC, LCMS). To the reaction was then added water, and the resultant solid was filtered, washed with water and then dried. Reverse phase column chromatography (2:3, MeCN:H<sub>2</sub>O) afforded the title compound as a white solid (76 mg, 0.164 mmol, 43%).

$^1\text{H}$  NMR (600 MHz, DMSO- $d_6$ )  $\delta$ /ppm: 9.86 (m, 1H), 8.08 (m, 1H), 7.71-7.44 (m, 5H), 7.30-7.25 (m, 2H), 7.24-7.16 (m, 3H), 4.59 (m, 1H), 2.82 (m, 1H), 2.72 (m, 1H), 2.02 (m, 3H), 1.31 (m, 9H).

$^{13}\text{C}$  NMR (150 MHz, DMSO- $d_6$ )  $\delta$ /ppm: 170.1, 167.9, 165.5, 164.5, 134.7, 134.2, 129.2, 128.31, 128.27, 126.3, 126.2, 120.3, 119.3, 119.0, 79.9, 49.0, 27.7, 27.6, 24.0, 23.9.

LCMS [M+H] Calcd. for  $\text{C}_{25}\text{H}_{31}\text{N}_6\text{O}_3^+$  463.24; measured 463.30

**tert-butyl (S)-3-((4-((4-acetamidophenyl)amino)-1,3,5-triazin-2-yl)amino)-5-phenylpentanoate (45)**

To a solution of **30** (96 mg, 0.364 mmol) and *tert*-Butyl homophenylalanine (100 mg, 0.401 mmol) in dry DMF (2 mL) at r.t. was added triethylamine (0.061 mL) and the mixture stirred at 80°C for 3h (TLC, LCMS). To the reaction was then added water, and the resultant solid was filtered, washed with water and then dried. Column chromatography (19:1, CH<sub>2</sub>Cl<sub>2</sub>:MeOH) followed by reverse phase column chromatography (1:1, MeCN:H<sub>2</sub>O) afforded the title compound as a white solid (0.041 g, 0.089 mmol, 24%).

$^1\text{H}$  NMR (600 MHz, DMSO- $d_6$ )  $\delta$ /ppm: 9.85 (m, 1H), 8.15 (s, 1H), 7.57 (m, 2H), 7.50 (m, 2H), 7.31-7.16 (m, 5H), 4.24 (m, 1H), 2.75 (m, 1H), 2.68 (m, 1H), 2.02 (s, 3H), 1.39 (s, 3H), 1.33 (s, 6H).

$^{13}\text{C}$  NMR (150 MHz, DMSO- $d_6$ )  $\delta$ /ppm: 172.0, 167.9, 165.5, 165.1, 141.1, 134.6, 134.2, 128.5, 128.4, 126.0, 119.3, 119.0, 80.6, 32.8, 31.9, 31.7, 27.8, 27.7, 27.6, 24.0, 23.8.

LCMS [M-H] Calcd. for  $\text{C}_{26}\text{H}_{31}\text{N}_6\text{O}_3^-$  463.24; measured: 463.30

**(S)-N-(4-((4-((1-(*tert*-butoxy)-4-methylpentan-2-yl)amino)-1,3,5-triazin-2-yl)amino)phenyl)acetamide (46)**

To a solution of **33** (20 mg, 0.058 mmol) and molecular sieves and MTBE (0.5 mL) was added dropwise conc. sulfuric acid (10  $\mu\text{L}$ , 0.174 mmol) and the reaction stirred at r.t. for 5h. Once the starting material had fully dissolved, the reaction was then slowly quenched with saturated aqueous solution of sodium bicarbonate. Organic layer was separated, and aqueous layer was extracted twice with ethyl acetate. The combined organic layers were washed with water, dried over magnesium sulfate and the solvent was removed *in vacuo*. Column chromatography (19:1, CH<sub>2</sub>Cl<sub>2</sub>:MeOH) afforded the title compound as a white solid (0.004 g, 0.0099 mmol, 17%).



<sup>1</sup>H NMR (600 MHz, DMSO-d<sub>6</sub>) δ/ppm: 9.83 (s, 1H), 9.45 (m, 1H), 7.70-7.61 (m, 2H), 7.46 (dd, 2H, J = 8.9, 2.0 Hz), 7.30 (s, 1H), 4.10 (s, 1H), 3.18 (m, 1H), 2.01 (s, 3H), 1.63 (m, 1H), 1.43-1.39 (m, 2H), 1.11 (s, 9H), 0.88 (d, 2H, J = 6.7 Hz), 0.85-0.81 (m, 3H).

LCMS [M+H] Calcd. for C<sub>21</sub>H<sub>33</sub>N<sub>6</sub>O<sub>2</sub><sup>+</sup> 401.26; measured: 401.30.

#### **(4-((4-acetamidophenyl)amino)-1,3,5-triazin-2-yl)-L-phenylalanine (47)**

To a suspension of **41** (20 mg, 0.045 mmol) in DCM (2 mL) at room temperature was added trifluoroacetic acid (0.4 mL) and the mixture stirred at room temperature for 18h. The solvent was then removed *in vacuo* and the residue triturated with *i*Pr<sub>2</sub>O. The solid formed was collected by filtration, azeotroped with dichloroethane and dried to afford the title compound (15 mg, 0.041 mmol, 91 %).

<sup>1</sup>H NMR (600 MHz, DMSO-d<sub>6</sub>) δ/ppm: 9.85 (m, 1H), 8.14 (s, 1H), 7.53 (d, 2H, J = 8.4 Hz), 7.48 (dd, 2H, J = 9.5, 2.7 Hz), 7.31-7.25 (m, 4H), 7.19 (m, 1H), 4.58 (m, 1H), 3.16 (m, 1H), 3.03 (m, 1H), 2.01 (m, 3H).

LCMS [M+H] Calcd. for C<sub>20</sub>H<sub>21</sub>N<sub>6</sub>O<sub>3</sub><sup>+</sup> 393.16; measured: 393.20.

#### **SPR assay**

All SPR analysis was performed on a BIAcore T200 system using Series S CM5 sensor chips. All sensorgrams were double-referenced by subtracting the response on a reference flow cell and a blank sample. Ligands were evaluated against the FL (27–541) NPR-C Protein. Human FL NPR-C (27–541)-10His-Flag were covalently attached to a CM5 chip via amine coupling<sup>14</sup> with a surface density of 5,000 RU. Binding of agonists (150 μM to 0 μM) was analysed by multi-cycle sequential injections at a flow rate of 30 μl/min (60s association time) followed by undisturbed dissociation (30s) during which curves returned to baseline. Peptide antagonist M372049 was used as a positive control. Agonists were dissolved in DMSO and the final sample solutions for kinetic affinity assays were 1% DMSO in 1X phosphate buffered salineP20 buffer (PBS-P, Cat no 28995084, GE Healthcare Ltd.). DMSO solvent effects were corrected for with eight calibration solutions (0.5%–1.8% DMSO in PBS-P). Equilibrium constants (KD) were calculated using the affinity model, assuming simple 1:1 (Langmuir) binding. Data processing and analysis were performed using BIAevaluation and OriginPro software. The theoretical R<sub>max</sub> (the maximal feasible signal between a ligand–analyte pair) for each compound/protein pair was calculated using Equation (1):<sup>35</sup>

$$R_{max} = R_{ligand} \cdot \left( \frac{Mr_{analyte}}{Mr_{ligand}} \right) \cdot V_{ligand} \quad (1)$$

where R<sub>ligand</sub>, amount of protein loaded in the SPR chip in response units; Mr<sub>analyte</sub>, molecular weight of the compound of interest; Mr<sub>ligand</sub>, molecular weight of the immobilized protein; V<sub>ligand</sub>, stoichiometry of the binding interaction between the ligand and the analyte. The experimentally observed R<sub>max</sub> was then calculated as a percentage of the theoretical R<sub>max</sub> as a quality control measure. An experimental R<sub>max</sub> <100% of the theoretical R<sub>max</sub> was considered sensible and indicative of genuine binding.<sup>35</sup>

#### **FP assay**

All experiments were performed using PBS-P buffer, a 100 μL final volume and 1% DMSO. Protein titration experiments were performed at 1.5, 15, 150 and 1500 pM P19 probe concentration. To achieve a balance of protein consumption and fluorescence polarization dynamic read-out range for competition experiments, the concentrations selected were 20 nM protein concentration and 150

pM P19 probe concentration. Keeping the appropriate reaction plate or tubes on ice, the optimized fluorescence polarization samples were prepared in the following order – ligand in PBS-P-4% DMSO (2400-1.097  $\mu$ M, 25  $\mu$ L), NPR-C protein in PBS-P buffer (128 nM, 25  $\mu$ L) and P19 probe in PBS-P buffer (300 pM, 50  $\mu$ L). Fluorescence polarization competition experiments against the Flu-P19 probe were performed with varying concentrations of ligand (600  $\mu$ M – 0.274  $\mu$ M) and their fluorescence polarization readout measured and normalized to experimental controls (buffer+probe, protein+probe) using a BMG Labtech Omega Pherastar<sup>®</sup> plate reader (filter settings: 485nm [excitation] and 520 nm [emission]). Background fluorescence polarization was blanked using a PBS-P-1% DMSO buffer only control. Raw data were processed using OriginPro curve fitting software to obtain the EC<sub>50</sub>s.

### **Organ Bath**

The vascular reactivity of rat thoracic aortic and murine mesenteric arterial (from wild type and NPR-C<sup>-/-</sup> animals) vascular ring preparations was determined using classical tissue bath pharmacology, as we have described previously.<sup>36</sup> To confirm the specific NPR-C response on rat small mesenteric artery, some vessels were incubated with M372049 (10  $\mu$ M) or osteocrin (100 nM) for 15 min prior to test the vasorelaxant properties of the compounds. All studies conformed to the UK Animals (Scientific Procedures) Act of 1986 and had approval from a local Animal Welfare and Ethical Review Body.

### **HeLa Assay**

HeLa cells were selected to test NPR-C activation *in vitro* due to its higher expression of NPR-C over NPR-A or NPR-B.<sup>37</sup> Cells were maintained in DMEM high glucose media supplemented with 10% heat inactivated bovine serum, 100 U/mL penicillin and 100 U/mL streptomycin in a humidified incubator at 5% (v/v) CO<sub>2</sub>.

NPR-C contains a G<sub>i</sub> binding domain that upon activation of the receptor reduces cAMP synthesis by inhibiting adenylyl cyclase activity.<sup>6</sup> The ability of NPR-C agonists to inhibit forskolin-induced cAMP production was tested in 80% confluent HeLa cells.

On the assay day, media was changed and cells were left to stabilise for 4h. Cultures were pre-incubated with the NPR-C selective agonist cANF<sup>4-23</sup> (100 nM) or **1** (100  $\mu$ M) for 10 min prior to the addition of forskolin (10  $\mu$ M). 3-isobutyl-1-methylxanthine (IBMX, 1 mM) was added alongside the agonists to prevent cAMP degradation. In some experiments, to test the specificity of the agonism, cells were treated with the NPR-C antagonists osteocrin (100 nM) or M372049 (10  $\mu$ M) for 10 min prior to the addition of the agonists. After 20 min of forskolin activation, cells were lysated in 1% triton-X/1M HCl buffer, spun at 14000 rpm for 2 min at 4°C and supernatants frozen for further analyses. The supernatants thereby obtained were used for cAMP measurements using an ELISA kit as instructed by the manufacturer (Enzo Life Sciences, Farmingdale, USA) and normalised to the protein concentration of the sample measured by BCA protein assay (Thermo Scientific, MA, USA).

### **ADME and PK data**

Determination of ADME and PK parameters (clearance and half-life in rat hepatocyte and human plasma, plasma protein binding, cyp P450 inhibition, and *in vivo* studies) were conducted by WuXi AppTech.

### **Plasma Protein Binding**

Binding of compounds and warfarin (positive control) to human and SD rat plasma protein was determined using equilibrium dialysis, the concentration of analyte was determined by using the

peak area ratio of analyte and internal standard. The results were calculated using the following equations:

$$\% \text{ Unbound} = 100 * F_c / T_c, \% \text{ Bound} = 100 * (1 - F_c / T_c)$$

$$\% \text{ Recovery} = 100 * (F_c + T_c) / T_0$$

$T_c$  = Total compound concentration as determined by the calculated concentration on the retentate side of the membrane

$F_c$  = Free compound concentration as determined by the calculated concentration on the dialysate side of the membrane

$T_0$  = Total compound concentration as determined before dialysis

### Stability in Rat hepatocyte

Cryopreserved rat hepatocytes were tested for cell viability with trypan blue and found to be 80 % viable (vendor: BioreclamationIVT; Cat. No. M00005; lot. BSI; pooled of 27 male SD rats).

Test compounds were provided as a 10 mM stock in DMSO, 30 mM stock solutions of positive control compounds in DMSO were prepared.

1. 1000x stock was prepared by dilution of 10 mM and 30 mM stock solution to 1 mM and 3 mM respectively with DMSO in a 96 well plate.
2. 50x intermediate solution: 20  $\mu$ L of 1000x stock solution was pipetted and mixed with 380  $\mu$ L of 45 % MeOH/H<sub>2</sub>O to obtain 50  $\mu$ M and 150  $\mu$ M stock solutions.
3. 5x working solution: 50  $\mu$ L of 50x intermediate stock solution was pipetted and mixed with 450  $\mu$ L pre-warmed Williams' medium E to obtain 5  $\mu$ M and 15  $\mu$ M test and control compound solutions respectively.
4. Spiked 10  $\mu$ L of 5x Working Solution into appropriate wells in 96-well plates corresponding to T<sub>0</sub>, T<sub>15</sub>, T<sub>30</sub>, T<sub>60</sub> and T<sub>90</sub> in duplicates. All pre-labelled plates with compounds were kept warm in an incubator at 37°C.
5. Preparation of 0.625x10<sup>6</sup>/mL cells suspension: cryopreserved cells were thawed, isolated and suspended in Williams' Medium E, then diluted with pre-warmed Williams' Medium E to 0.625 × 10<sup>6</sup> cells/mL.
6. The reaction was started by aliquoting 40  $\mu$ L of 0.625x10<sup>6</sup>/mL cells suspension into each well in 96-well plates containing 10  $\mu$ L compounds to obtain a final concentration of 1  $\mu$ M test compound and 3  $\mu$ M control compound.
7. For T<sub>15</sub>, T<sub>30</sub>, T<sub>60</sub> and T<sub>90</sub> sample plates were incubated immediately in an incubator at 37°C with 5% CO<sub>2</sub>. T<sub>0</sub> samples were added stop solution before adding the cells.
8. Medium Control (MC) Sample Plates (T<sub>0</sub>-MC and T<sub>90</sub>-MC): T<sub>0</sub>-MC and T<sub>90</sub>-MC sample plates were incubated as the same condition above at the T<sub>0</sub> and T<sub>90</sub> with Williams' Medium E only without cells.
9. At each corresponding time point reaction was stopped by quenching with ACN containing internal standards (IS) at 1:3 ratio.
10. Vortexed sample plates immediately and placed on a plate shaker at 500 rpm for 10 min, then centrifuged at 3220 × g for 20 min.
11. The supernatants were transferred to another set of pre-labelled 96-deep-well plates which contain appropriate dilution solution. The plates were sealed and stored at 4°C until LC-MS-MS analysis.

The remaining percent of test articles after incubation were calculated by the follow equation:

**% Remaining (at Appointed Time) =**

$$\frac{\text{Peak Area Ratios of Test Article versus Internal Standard at Appointed Time}}{\text{Peak Area Ratios of Test Article versus Internal Standard at } 0 \text{ min}} \times 100\%$$

### Human plasma stability assay:

10 mM stock solutions of the control and test compounds in DMSO were prepared. Pooled human plasma (EDTA-K2, bioreclamationIVT, cat# HMPLEDTA2, batch BRH1274040) was used in this assay with minimum number of individuals 3 male and 3 female.

1. The pooled frozen plasma was thawed in a water bath at 37°C prior to experiment, plasma was centrifuged at 4000 rpm and the clots (if any) were removed. The pH was adjusted to  $7.4 \pm 0.1$  if required.
2. 1mM intermediate solution was prepared by diluting 10  $\mu$ L stock solution with 90  $\mu$ L DMSO, 1 mM positive control propantheline was prepared by diluting 5  $\mu$ L stock with 35  $\mu$ L ultra-pure water, 1 mM intermediate solution of the positive control enalapril was prepared by diluting 5  $\mu$ L stock with 45  $\mu$ L DMSO.
3. 100  $\mu$ M dosing solution was prepared by diluting 20  $\mu$ L of intermediate solution with 180  $\mu$ L 45% MeOH/H<sub>2</sub>O. Propantheline and enalapril were prepared by diluting 10  $\mu$ L of the intermediate solution with 90  $\mu$ L 45 % MeOH/H<sub>2</sub>O.
4. 196  $\mu$ L of blank plasma was spiked with 4  $\mu$ L of dosing solution to achieve 2  $\mu$ M of the final concentration in duplicate, and samples were incubated at 37°C in a water bath.
5. At each time point (0, 10, 30, 60 and 120 minutes) 800  $\mu$ L of stop solution (200 ng/mL tolbutamide and 200 ng/mL labetalol in 50% CAN/MeOH) was added to precipitate protein and mix thoroughly.
6. Centrifuged sample plates at 4000 rpm for 10 minutes. An aliquot of supernatant (100  $\mu$ L) was transferred from each well and mixed with 200  $\mu$ L ultra-pure water. The samples were shaken at 800 rpm for 10 minutes before submitting to LC-MS/MS analysis.

### Data analysis

The % remaining of test compound after incubation in plasma was calculated using the following equation:

$$\% \text{ remaining} = 100 \times (\text{PAR at appointed incubation time} / \text{PAR at } T_0)$$

Where PAR is the peak area ratio of analyte vs. internal standard.

### CYP P450 inhibition

Working solutions (100x) of the test compounds in 1:1 DMSO:MeOH were prepared by dilution of stock solutions in DMSO to provide working concentration ranges of 5 mM, 1.5 mM, 0.5 mM, 0.15 mM, 0.05 mM, 0.015 mM, and 0.005 mM.

Working solutions (100x) of the positive controls ( $\alpha$ -naphthoflavone, ticlopidine, montelukast, sulfaphenazole, (+)-N-3-benzylrivanol, quinidine and ketoconazole) were prepared in MeOH at 300  $\mu$ M concentration.

NADPH solution (10x) was prepared at a concentration of 10 mM with 33 mM MgCl<sub>2</sub> solution.

Human liver microsome working solution (1.27x) was prepared at a concentration of 0.127 mg/mL with PB.

Working solutions (10x) of CYP substrates were prepared with dilution from stocks with PB:

CYP	Substrate	Concentration ( $\mu$ M)
1A2	Phenacetin	750

2B6	Bupropion	800
2C8	Amodiaquine	20
2C9	Diclofenac	100
2C19	S-mephenytoin	200
2D6	Dextromethorphan	100
3A4	Midazolam	20
3A4	testosterone	400

1. Prepare test compound and standard inhibitor working solutions
2. Thaw microsomes on ice
3. Add 20 µL of the substrate solutions to corresponding wells, add 20 µL PB
4. Add 2 µL of the test compounds and positive control working solutions to the corresponding wells, add 2 µL solvent to no inhibitor and blank wells
5. Prepare HLM working solution
6. Add 158 µL of the HLM working solution to all wells of incubation plate
7. Pre warm plate for 10 minutes at 37°C water bath
8. Prepare NADPH cofactor solution
9. Add 20 µL NADPH cofactor to all incubation wells
10. Mix and incubate for 20 minutes for CYP2C19, CYP2D6, 3 minutes for 3A4 (midazolam) and 10 minutes for others at 37°C water bath
11. At the time point terminate the reaction by adding 400 µL cold stop solution (200 ng/mL tolbutamide and labetalol in acetonitrile)
12. The samples are centrifuged at 4000 rpm for 20 minutes to precipitate protein
13. Transfer 200 µL supernatant to 100 µL HPLC water and shake for 10 minutes
14. Samples are ready for LC/MS/MS analysis

#### Data analysis

SigmaPlot (V.11) used to plot % control activity versus the test compound concentrations, and for non-linear regression analysis of the data. IC50 values plotted using the equation:

$$y = \frac{max}{1 + \left(\frac{x}{IC50}\right)^{-hillslope}}$$

IC 50 values will be reported as >50 µM when % inhibition at highest concentration is less than 50%.

#### **PAMPA (Parallel artificial membrane permeability assay) Protocol**

Test compounds were loaded to the donor plate of the PAMPA sandwich system (Corning Gentest Pre-coated PAMPA Plate System®) using dimethyl sulfoxide (DMSO) and phosphate buffered saline (PBS) (pH 7.4) (5% DMSO, 100 µM, n=4), and the resultant wells thoroughly mixed. Two blanks (5% DMSO only) were included for each test compound. Prior to start of the experiment, an aliquot of each well was then transferred to a UV analysis plate containing acetonitrile (MeCN) for UV analysis of donor plate concentration at t= 0. PBS was then added to the acceptor plate, and the acceptor plate carefully lowered onto the donor plate, and the PAMPA plate assembly incubated at room temperature for 5h. At the end of incubation, aliquots from each well of the donor plates were transferred to a 96-well UV/VIS analysis plate containing MeCN and each well thoroughly mixed for UV analysis. Sample aliquots were also taken from the acceptor plate for LCMS analysis using single ion monitoring (SIM) for the m/z<sup>+</sup> and m/z<sup>-</sup> for each compound. The results obtained were then quantified against a standard curve for each test sample using either UV/VIS or LCMS SIM.

#### **Aqueous solubility**

All Test compounds were formulated in DMSO at a concentration of 10 mM. Reference controls were also formulated in DMSO as above. The following reference controls were used: Ketoconazole, nicardipine.HCl, tamoxifen.

Working solutions:

50 % PBS: 50 % acetonitrile (Working solution A)

47.5 % PBS: 47.5 % acetonitrile: 5% DMSO (Working solution B)

95 % PBS: 5 % DMSO (Working solution C)

**Solubility test:** Test compounds (12.5  $\mu$ l; 10 mM) were added to PBS (237.5  $\mu$ l) in quadruplicate in a 96-well plate. The wells were mixed (10 times using a 100 $\mu$ l mixing volume), a cover slip sealed on the plate, and plate shaken at 700 rpm at room temperature for 3h. 250 $\mu$ l from each well was then transferred to a Merck filtration plate (Product code: MSRLN0410), and the filtration plate placed on the Merck/Supelco vacuum manifold (Product code: 575650-U) and filtered under vacuum, and the filtrate collected into a Merck 96-deep well plate (product code: AXYPDW20CS). Acetonitrile (50 $\mu$ l) was dispensed into clean high sensitivity 96-well UV/VIS Corning analysis plate (Product code: CLS3635) and the aqueous filtrate (50  $\mu$ l) transferred from the collection wells to UV analysis plate. The wells were mixed the plate analysed at the  $\lambda_{\max}$  specific to each compound. Two blanks (50 $\mu$ l MeCN + 50 $\mu$ l Working solution C) were included for each test compound. The results obtained were quantified against a standard calibration curve prepared for each test sample as described below.

#### **Calibration curve construction:**

The following procedure was completed on an Apricot automatic pipettor:

Test compound (7.5 $\mu$ l; 10 mM) was added in duplicate to working solution A (142.5 $\mu$ l) to give a 500  $\mu$ M stock concentration. This stock solution was serially diluted (4 three-fold dilutions) by adding 50  $\mu$ l to working solution B (100  $\mu$ l) until a final concentration of 6.17  $\mu$ M was achieved (5 concentrations, 6 compounds, n=2). The stock solution was mixed 10 times with 100 $\mu$ l mix volume (or until full dissolution occurred), while each dilution was mixed 5 times with 100 $\mu$ l mix volume. Two blanks (Working solution B only) were included for each compound. Samples were analysed using a BMG Labtech microplate reader first at the full spectrum 220-650nm) of wavelengths to determine the  $\lambda_{\max}$  specific to each compound, and then usually at the following wavelengths: 290, 300, 320, 340, 360nm.

#### **In vivo studies**

PK IV

Fasted, male C57BL/6 mice were treated with an intravenous dose of **1** (nominal dose 3.00 mg/Kg, administered dose 2.58 mg/Kg) formulated as a 1.00 mg/mL solution in 5% DMSO, 5% solutol and 90% water.

PK oral

Fasted, male C57BL/6 mice were treated with an PO dose of **1** (nominal dose 10.0 mg/Kg, administered dose 8.60 mg/Kg) formulated as a 1.00 mg/mL solution in 5% DMSO, 5% solutol and 90% water.

Plasma sample analysis:

Internal standard: 100 ng/mL Labetalol + 100 ng/mL dexamethasone + 100 ng/mL tolbutamide + 100 ng/mL verapamil + 100 ng/mL Glyburide + 100 ng/mL Celecoxib in acetonitrile

A calibration curve of **1** was established from 1 – 1000 ng/mL in male C57BL/6 mouse plasma (EDTA-K2)

An aliquot of 8  $\mu$ L sample was protein precipitated with 160  $\mu$ L IS, the mixture was vortex-mixed well and centrifuged at 10000 rpm for 20 min, 4°C. 4  $\mu$ L supernatant was injected for LC-MS/MS analysis.

### Figure legends.

Figure 1. Structures of NPR-C active peptides, and lead compound **1**; active CNP peptide displayed in red, brackets denote disulphide bonds.

Figure 2. Peptidomimetic ligand active against NPR-C.

Figure 3. Small Molecule NPR-A and NPR-C agonists

Figure 4. reversal of agonist induced vasorelaxation upon treatment with NPR-C inhibitors in rat small mesenteric artery. A The selective NPR-C peptide agonist cANF<sup>4-23</sup> causes vasorelaxation that is blocked by M372049 and osteocrin; B small molecule agonist **1** causes vasorelaxation that is partially blocked by M372049 and osteocrin.

Figure 5. Evaluation of NPR-C agonism in HeLa cells by a cAMP assay. A cANF<sup>4-23</sup> inhibits cAMP formation that is reversed by M372049 and osteocrin; B small molecule agonist **1** modestly inhibits cAMP formation that is reversed by M372049 and osteocrin; C M372049 and osteocrin do not affect basal forskolin-induced cAMP production.

Scheme 1. Synthesis of 1,4-cyclohexane disubstituted bis-triazine and monomeric chlorotriazine derivatives.

Scheme 2. Synthesis of L-valine triazine derivatives

Scheme 3. Synthesis of amino acid substituted triazines.

### Associated Content

Supporting Information

Surface Plasmon Resonance Sensorgrams and Affinity Dose-Response Plots for **1** and **26**. LCMS chromatograms and ESI mass spectra for compounds **1**, **17**, **19-22**, **25-29**, **32-47**.

### Corresponding Author

\* Professor David Selwood, Wolfson Institute for Biomedical Research, University College London Cruciform Building, Gower St, London WC1E 6BT, UK. Email: [d.selwood@ucl.ac.uk](mailto:d.selwood@ucl.ac.uk).

\* Professor Adrian Hobbs, William Harvey Research Institute, Barts & The London School of Medicine, Queen Mary University of London, Charterhouse Square, London EC1M 6BQ, UK. Email: [a.j.hobbs@qmul.ac.uk](mailto:a.j.hobbs@qmul.ac.uk).

### Author Contributions

All authors have given approval to the final version of the manuscript. †These authors contributed equally.

## Notes.

The authors declare no competing financial interests.

## Acknowledgements

This research was funded by the British Heart Foundation (BHF) Translational Award (TG/15/3/31692).

## References

1. Potter, L. R.; Yoder, A. R.; Flora, D. R.; Antos, L. K.; Dickey, D. M., Natriuretic peptides: their structures, receptors, physiologic functions and therapeutic applications. *Handb Exp Pharmacol* **2009**, (191), 341-366.
2. Kuhn, M., Molecular Physiology of Membrane Guanylyl Cyclase Receptors. *Physiological Reviews* **2016**, *96* (2), 751-804.
3. Chinkers, M.; Garbers, D. L.; Chang, M.-S.; Lowe, D. G.; Chin, H.; Goeddel, D. V.; Schulz, S., A membrane form of guanylate cyclase is an atrial natriuretic peptide receptor. *Nature* **1989**, *338* (6210), 78-83.
4. Schulz, S.; Singh, S.; Bellet, R. A.; Singh, G.; Tubb, D. J.; Chin, H.; Garbers, D. L., The primary structure of a plasma membrane guanylate cyclase demonstrates diversity within this new receptor family. *Cell* **1989**, *58* (6), 1155-1162.
5. Chauhan, S. D.; Nilsson, H.; Ahluwalia, A.; Hobbs, A. J., Release of C-type natriuretic peptide accounts for the biological activity of endothelium-derived hyperpolarizing factor. *Proceedings of the National Academy of Sciences* **2003**, *100* (3), 1426.
6. Anand-Srivastava, M. B., Natriuretic peptide receptor-C signaling and regulation. *Peptides* **2005**, *26* (6), 1044-1059.
7. Moyes, A. J.; Khambata, R. S.; Villar, I.; Bubb, K. J.; Baliga, R. S.; Lumsden, N. G.; Xiao, F.; Gane, P. J.; Rebstock, A.-S.; Worthington, R. J.; Simone, M. I.; Mota, F.; Rivilla, F.; Vallejo, S.; Peiró, C.; Sánchez Ferrer, C. F.; Djordjevic, S.; Caulfield, M. J.; MacAllister, R. J.; Selwood, D. L.; Ahluwalia, A.; Hobbs, A. J., Endothelial C-type natriuretic peptide maintains vascular homeostasis. *The Journal of Clinical Investigation* **2014**, *124* (9), 4039-4051.
8. Maack, T.; Suzuki, M.; Almeida, F. A.; Nussenzveig, D.; Scarborough, R. M.; McEnroe, G. A.; Lewicki, J. A., Physiological role of silent receptors of atrial natriuretic factor. *Science* **1987**, *238* (4827), 675.
9. Moyes, A. J.; Chu, S. M.; Aubdool, A. A.; Dukinfield, M. S.; Margulies, K. B.; Bedi, K. C., Jr.; Hodivala-Dilke, K.; Baliga, R. S.; Hobbs, A. J., C-type natriuretic peptide co-ordinates cardiac structure and function. *European Heart Journal* **2019**, *41* (9), 1006-1020.
10. Egom, E. E.; Vella, K.; Hua, R.; Jansen, H. J.; Moghtadaei, M.; Polina, I.; Bogachev, O.; Hurnik, R.; Mackasey, M.; Rafferty, S.; Ray, G.; Rose, R. A., Impaired sinoatrial node function and increased susceptibility to atrial fibrillation in mice lacking natriuretic peptide receptor C. *The Journal of Physiology* **2015**, *593* (5), 1127-1146.
11. Potter, L. R.; Abbey-Hosch, S.; Dickey, D. M., Natriuretic Peptides, Their Receptors, and Cyclic Guanosine Monophosphate-Dependent Signaling Functions. *Endocrine Reviews* **2006**, *27* (1), 47-72.
12. Millar, J. C.; Savinainen, A.; Josiah, S.; Pang, I.-H., Effects of TAK-639, a novel topical C-type natriuretic peptide analog, on intraocular pressure and aqueous humor dynamics in mice. *Exp Eye Res* **2019**, *188*, 107763.
13. Edelson, J. D.; Makhlina, M.; Silvester, K. R.; Vengurlekar, S. S.; Chen, X.; Zhang, J.; Koziol-White, C. J.; Cooper, P. R.; Hallam, T. J.; Hay, D. W. P.; Panettieri, R. A., In vitro and in vivo pharmacological profile of PL-3994, a novel cyclic peptide (Hept-cyclo(Cys-His-Phe-d-Ala-Gly-Arg-d-Nle-Asp-Arg-Ile-Ser-Cys)-Tyr-[Arg mimetic]-NH<sub>2</sub>) natriuretic peptide receptor-A agonist that is



- resistant to neutral endopeptidase and acts as a bronchodilator. *Pulmonary Pharmacology & Therapeutics* **2013**, *26* (2), 229-238.
14. Lisy, O.; Huntley, B. K.; McCormick, D. J.; Kurlansky, P. A.; Burnett, J. C., Design, Synthesis, and Actions of a Novel Chimeric Natriuretic Peptide: CD-NP. *Journal of the American College of Cardiology* **2008**, *52* (1), 60-68.
  15. Villar, I. C.; Panayiotou, C. M.; Sheraz, A.; Madhani, M.; Scotland, R. S.; Nobles, M.; Kemp-Harper, B.; Ahluwalia, A.; Hobbs, A. J., Definitive role for natriuretic peptide receptor-C in mediating the vasorelaxant activity of C-type natriuretic peptide and endothelium-derived hyperpolarising factor. *Cardiovascular Research* **2007**, *74* (3), 515-525.
  16. Veale, C. A.; Alford, V. C.; Aharony, D.; Banville, D. L.; Bialecki, R. A.; Brown, F. J.; Damewood, J. R.; Dantzman, C. L.; Edwards, P. D.; Jacobs, R. T.; Mauger, R. C.; Murphy, M. M.; Palmer, W. E.; Pine, K. K.; Rumsey, W. L.; Garcia-Davenport, L. E.; Shaw, A.; Steelman, G. B.; Surian, J. M.; Vacek, E. P., The discovery of non-basic atrial natriuretic peptide clearance receptor antagonists. Part 1. *Bioorg. Med. Chem. Lett.* **2000**, *10* (17), 1949-1952.
  17. Namikawa, K.; Shimamoto, T.; Kitano, K.; Koyama, Y. New imidazolone compound. 2008.
  18. Iwaki, T.; Nakamura, Y.; Tanaka, T.; Ogawa, Y.; Iwamoto, O.; Okamura, Y.; Kawase, Y.; Furuya, M.; Oyama, Y.; Nagayama, T., Discovery and SAR of a novel series of Natriuretic Peptide Receptor-A (NPR-A) agonists. *Bioorganic & Medicinal Chemistry Letters* **2017**, *27* (21), 4904-4907.
  19. Iwaki, T.; Oyama, Y.; Tomoo, T.; Tanaka, T.; Okamura, Y.; Sugiyama, M.; Yamaki, A.; Furuya, M., Discovery and dimeric approach of novel Natriuretic Peptide Receptor A (NPR-A) agonists. *Bioorganic & Medicinal Chemistry* **2017**, *25* (6), 1762-1769.
  20. Iwaki, T.; Tanaka, T.; Miyazaki, K.; Suzuki, Y.; Okamura, Y.; Yamaki, A.; Iwanami, M.; Morozumi, N.; Furuya, M.; Oyama, Y., Discovery and in vivo effects of novel human natriuretic peptide receptor A (NPR-A) agonists with improved activity for rat NPR-A. *Bioorganic & Medicinal Chemistry* **2017**, *25* (24), 6680-6694.
  21. Armistead, D. M.; Bemis, J. E.; Buchanan, J. L.; Dipietro, L. V.; Elbaum, D.; Geuns-Meyer, S. D.; Habgood, G. J.; Kim, J. L.; Marshall, T. L.; Novak, P. M.; Nunes, J. J.; Patel, V. F.; Toledo-Sherman, L. M.; Zhu, X. Preparation of 1,3,5-triazines as kinase inhibitors for treatment of angiogenesis or vasculogenesis. US20040116388A1, 2004.
  22. Li, Z.; Zou, H.; Zhu, W.; Shen, C.; Wang, R.; Liu, W.; Chen, X.; Tsui, H.; Yang, Z.; Zhang, X. Aminotriazines and related compounds as ErbB/BTK inhibitors and their preparation. WO2019149164A1, 2019.
  23. Likubo, K.; Kondoh, Y.; Shimada, I.; Matsuya, T.; Mori, K.; Ueno, Y.; Okada, M., Discovery of N-[2-Methoxy-4-[4-(4-methylpiperazin-1-yl)piperidin-1-yl]phenyl]-N'[2-(propane-2-sulfonyl)phenyl]-1,3,5-triazine-2,4-diamine (ASP3026), a Potent and Selective Anaplastic Lymphoma Kinase (ALK) Inhibitor. *Chem. Pharm. Bull.* **2018**, *66* (3), 251-262.
  24. Ruehter, G.; Koch, U.; Nussbaumer, P.; Schultz-Fademrecht, C.; Eickhoff, J. Pharmaceutically active disubstituted triazine derivatives. WO2012117048A1, 2012.
  25. Venkatraj, M.; Arien, K. K.; Heeres, J.; Joossens, J.; Dirie, B.; Lyssens, S.; Michiels, J.; Cos, P.; Lewi, P. J.; Vanham, G.; Maes, L.; Van der Veken, P.; Augustyns, K., From human immunodeficiency virus non-nucleoside reverse transcriptase inhibitors to potent and selective antitrypanosomal compounds. *Bioorg. Med. Chem.* **2014**, *22* (19), 5241-5248.
  26. Wu, Y. Preparation of triazine derivatives as anaplastic lymphoma kinase inhibitors. CN106146478A, 2016.
  27. Marugan, J. J.; Xiao, J.; Titus, S. A.; Southall, N.; Zheng, W.; Androphy, E. J.; Cherry, J. Preparation of arylthiazolylpiperidine derivatives and analogs for use as survival motor neuron (SMN) protein production modulators. WO2011130515A1, 2011.
  28. Salituro, F.; Farmer, L.; Wang, T.; Wang, J.; Bethiel, R.; Wannamaker, M.; Martinez-Botella, G.; Duffy, J.; Aronov, A.; Lauffer, D.; Pierce, A. Deazapurines useful as inhibitors of janus kinases and their preparation, pharmaceutical compositions and use in the treatment of various diseases. WO2007041130A2, 2007.

29. Lovett, J. A.; Portoghese, P. S., Synthesis and evaluation of melphalan-containing N,N-dialkylphenethylamine analogs as irreversible antagonists of the  $\delta$  opioid receptor. *J. Med. Chem.* **1987**, *30* (9), 1668-74.
30. Chen, M.-Y.; Lee, A. S.-Y., A simple and efficient esterification method. *J. Chin. Chem. Soc. (Taipei, Taiwan)* **2003**, *50* (1), 103-108.
31. Conole, D.; Myers, S. H.; Mota, F.; Hobbs, A. J.; Selwood, D. L., Biophysical screening methods for extracellular domain peptide receptors, application to natriuretic peptide receptor C ligands. *Chemical Biology & Drug Design* **2019**, *93* (6), 1011-1020.
32. Thakur, M.; Thakur, A.; Khadikar, P. V.; Supuran, C. T., QSAR study on pKa vis-a-vis physiological activity of sulfonamides: a dominating role of surface tension (inverse steric parameter). *Bioorg. Med. Chem. Lett.* **2005**, *15* (1), 203-209.
33. Wang, D.; Cai, Q.; Ding, K., An Efficient Copper-Catalyzed Amination of Aryl Halides by Aqueous Ammonia. *Adv. Synth. Catal.* **2009**, *351* (11+12), 1722-1726.
34. Wu, X.; Hu, L., Efficient amidation from carboxylic acids and azides via selenocarboxylates: application to the coupling of amino acids and peptides with azides. *J. Org. Chem.* **2007**, *72* (3), 765-774.
35. Biacore, A. B.; July, E.; Biacore, A. B., *BIAevaluation Software Handbook (3rd Ed)*. Biacore AB: Uppsala, 1997.
36. Villar, I. C.; Bubb, K. J.; Moyes, A. J.; Steiness, E.; Gulbrandsen, T.; Levy, F. O.; Hobbs, A. J., Functional pharmacological characterization of SER100 in cardiovascular health and disease. *Br. J. Pharmacol.* **2016**, *173* (23), 3386-3401.
37. Ali, A. A. Characterization of NPRC and its Binding Partners. A dissertation submitted in partial fulfillment of the requirements for the degree of Doctor of Philosophy. University of South Florida, Tampa, Florida, 2009.

Table of Contents Graphic

